MSc Thesis

# Fiber Reinforced Cementitious Composite Tailoring through 3D Lattice Fracture Simulations

Herry Prabowo

Delft University of Technology

July 2009

## STRUCTURAL ENGINEERING IS:

**THE ART OF USING MATERIALS** *That Have Properties Which Can Only Be Estimated*

**TO BUILD REAL STRUCTURES** *That Can Only Be Approximately Analyzed*

**TO WITHSTAND FORCES** *That Are Not Accurately Known*

**SO THAT OUR RESPONSIBILITY WITH RESPECT TO PUBLIC SAFETY IS SATISFIED**

(*Adapted From An Unknown Author*)

When one has a good understanding of the problem, one must rid it of all the superfluous concepts and reduce it to the simplest elements.
**(Rene Descartes 1596 - 1650)**

## Acknowledgements

First of all, I would like to express my gratitude to Prof. dr. ir. Klaas van Breugel who gave me a chance to carry out my MSc Thesis at the Microlab, Faculty of Civil Engineering and Geosciences, Delft University of Technology, the Netherlands.

I really appreciate my daily supervisors Dr. ir. H.E.J.G. Schlangen and ir. Zhiwei Qian for their kind supervisions and discussions through out the research.

Dr. ir. P.C.J. Hoogenboom from structural mechanics group is also appreciated for his valuable comments on the project.

The coordinator for Structural Engineering track Ir. Lambert Houben managed the issues concerning graduation.

Last but not least, the encouragements and supports from my family and friends are highly appreciated.

**Herry Prabowo**

Delft, July 2009

# Table of Contents

# Chapter 1 Introduction

## 1.1. Motivation

Concrete is currently the most used man-made material in the world. Even if the consumption of all other materials are combined, the amount of concrete consumed is still twice larger [1]. As of 2008, about 2.5 billion metric tons are made each year, equal to 369 kg for every person on earth [2]. No other material except water is consumed in such remarkable amounts [3].

As structural material, concrete actually is less strong compare to other materials such as steel. Perhaps one will wonder why concrete is widely spread in structural applications. There are at least three main reasons. First, it has an excellent resistance to water. Second, it can be formed into various shapes and sizes. And last but not least, it is usually the cheapest and the most readily available material [4].

Besides the advantages mentioned above, concrete also has several shortcomings. One of them is its brittle nature. This brittle property can significantly limit the applicability of the material in structural applications. There are two primary reasons why brittle materials are undesirable. Firstly, failure without warning. Brittle materials usually fail by the sudden unstable propagation of pre-existing cracks, no warning is provided (e.g. no large deflection of structural components) before failure occurs. Secondly, low material reliability. The size of pre-existing cracks (which may form during processing, handling, or service) is difficult to control and usually varies significantly from one component to another. As a result, the strength of components made with the same brittle material under similar processes can be very different [5].

Besides that, the facts in the field show that many infrastructure problems and failures can be traced back to the cracking and brittle nature of concrete. It is no wonder that significant research efforts have gone into attempts to enhance the ductility of concrete materials. Current research shows that the most effective way of enhancing concrete ductility is by adding fibers [6]. The research advances in this field yield a class of ultra ductile fiber reinforced cementitious composites called ECC (Engineered Cementitious Composites). Occasionally, these materials exhibit an extremely high strain capacity of more than 6% and a distributed crack pattern with fine cracks under imposed deformation loading. These material behaviors are achieved through microstructures tailoring including matrix, fiber, and interface parameter [7].

## 1.2. Objectives

In this project, 3D lattice analysis have been done in order to simulate the behavior of fiber cement based material under single fiber tests, uni-axial tensile tests, and four point bending tests. The results are then compared with the experimental results to give an idea how to obtain correct parameters from the tests that are currently carried out in the Microlab. In addition, a procedure has been developed to design ductile fiber reinforced cementitious composite (DFRCC).

## 1.3. Overview

The work-plan for this project is as following.

a. Study literature and report on what has been done so far in analytical and experimental results of fiber cementitious composites.

b. Discussion of mix design, experimental procedures and measured properties with Post-docs and PhD students working on Fiber Concrete in Microlab.
c. Make use of different software tools that are developed for the lattice model in order to study the behavior of fiber concrete which include the variations of fiber dimensions (length and cross section), fiber mechanical properties (strength and stiffness), fiber bond properties (pull-out strength), fiber percentage, cement matrix properties (strength and stiffness).
d. Develop a procedure on how to obtain the right model parameters from the tests that are being performed in the laboratory.
e. Setting up of various simulations of tensile and bending tests on fiber concrete and performing experimental results comparison
f. Explanation of the design procedure in which the model is elaborated in clear steps in form of MSc Thesis report.

## 1.4. Outline of the thesis

The thesis is divided into six chapters.

Chapter 1 explains the motivation of this research and gives an overview of the current progress of fiber reinforced cementitious composite. The objective and overview of the thesis are given as well.

Chapter 2 introduces the concept of micromechanical design and its significant role in bridging the material composition and the structural performance (Integrated Structures and Materials Design approach).

Chapter 3 reviews the existing experimental and analytical results for single fiber test, uni-axial tensile test, and four point bending test.

Chapter 4 presents the results of 3D Lattice analysis simulation for single fiber test, uni-axial tensile test, and four point bending test.

Chapter 5 compares the results of the experimental and 3D Lattice analysis simulation for single fiber test, uni-axial tensile test, and four point bending test.

Chapter 6 concludes the major findings of the thesis, indicates the shortcomings of the results, and suggests possible further researches.

# Chapter 2 Micromechanics Based Design

This chapter is intended to give understanding of the important contribution of the micromechanical model to successfully design a ductile fiber reinforced cementitious composite. The current issue on design philosophy and cementitious materials classification are also incorporated.

## 2.1 Classification of cementitious materials

New materials make new promises with new terminologies. Until now, various composites have been developed towards their specific targets, and those targets were often explained with specific terminologies. DFRCC (Ductile Fiber Cementitious Composite) are no exceptions. DFRCC emphasize their differences from conventional cementitious materials such as concrete and fiber reinforced concrete. Therefore, DFRCC terminologies has to be prepared to explain those differences and to construct innovative structural application concepts. This classification is based on Matsumoto and Mihashi [8].

DFRCC (Ductile Fiber Reinforced Cementitious Composite) is a class of FRCC (Fiber Reinforced Cementitious Composite) that exhibit multiple cracking (Figure 1 and table 1). Multiple cracking leads to improvement in properties such as ductility, toughness, fracture energy, strain hardening, strain capacity, and defroamtion capacity under tension, compression, and bending. These improved properties of DFRCC have triggered unique and versatile structural applications/ concepts, including damage reduction, damage tolerance, energy absorption, crack distribution, deformation compatibility, delamination, and so on.

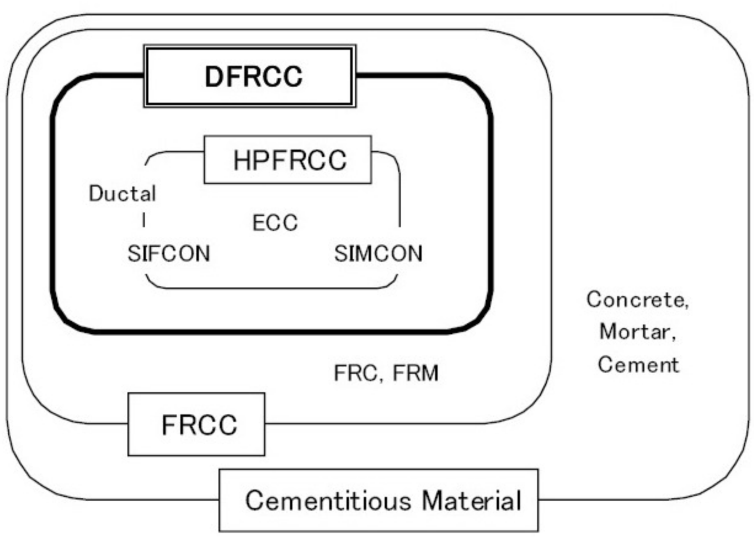


**Figure 2.1 Classification of cementitious materials**

| | Cement, mortar | Concrete, FRC | DFRCC | |
|---|---|---|---|---|
| | | | | HPFRCC |
| **Material response** | Brittle | Quasi brittle | Quasi brittle (tension) / Ductile (flexure) | Ductile |
| **Strain softening/ hardening** | - | Strain softening | Strain softening (tension) / hardening (flexure) | Strain Hardening |
| **Cracking behavior (flexure)*** | Localized cracking | Localized cracking | Multiple cracking | Multiple cracking |
| **Cracking behavior (tension)** | Localized cracking | Localized cracking | Localized cracking | Multiple cracking |

**Table 2.1 Characteristics of cementitious materials**

* Cracking behavior in flexure is dependent on specimen dimensions.

DFRCC is a broader class of materials than HPFRCC (High Performance Fiber Reinforced Composite). HPFRCC is an FRCC that shows multiple cracking and strain hardening in tension, and therefore in bending as well [9]. On the other hand, DFRCCC encompasses a group of FRCC that exhibit multiple cracking in bending only, in addition to HPFRCC. The focus on DFRCC is due to the need to generally explore the role of multiple cracking and the utilization of accompanying properties and structural applications/ concepts in this broad class of materials. With the broad scope and the basis on the accumulated knowledge in the research community, DFRCC studies are expected to lead to the development and evaluation of new materials, to the development of innovative structural applications/ concepts and to establish the relation between structural applications/ concepts and required material performance.

## 2.2 Performance based design concept (PBDC)

The responsibility of structural design community become greater as the structural design codes in many countries have moved or are moving towards performance based design conceptsin place of the classical prescriptive approach. The performance objectives may be specified in terms of operability, repairability, life safety, or collapse prevention subsequent to specified load level (see SEAOC 1995 for instance). The structural engineer therefore have to ensure that the structural design directly links to an expected outcome in performance [10].

The performance based design concept allows for greater flexibility, e.g., in dimensioning and reinforcement detailing by structural engineers. It also allows for a larger degree of freedom in construction material choice. To fully exploit this last aspect, it is desirable to have a larger repertoire of concrete materials, particularly those with properties drastically improved over the limitations of current concrete. Performance based design creates opportunities for collaboration between structural engineers and materials engineers.

In the domain of structural engineering, materials are shaped into structural elements that are then assembled into structural systems in order to meet targeted structural functions and performance goals. The performance goals are often stated in terms of ultimate limit states or serviceability limit states. Typically, design codes provide the structural design framework with respect to material selection, dimensioning, and in the case of reinforced concrete, reinforcement detailing.

Embodied within design codes are deep knowledge developed from structural mechanics analyses and verified by extensive experimental investigations and experience. Structural analyses utilize mechanical properties of materials in the form of constitutive laws. Thus structural mechanics forms the basic analytic tool for structural engineers. This body of knowledge while not visible to the eye, is the fundamental reason why structures (in most instances) carry anticipated loads in a predictable way. The world of structural engineering, shaping materials into structural elements and joining them to form structural systems, with structural performance as the target [11].

## 2.3 Performance driven design approach (PDDA)

The concept of Performance Driven Design Approach (PDDA) explained here is based on Li 1992 [12] proposed for fiber reinforced cementitious composites (FRCC). It is simply illustrated by the following figure.

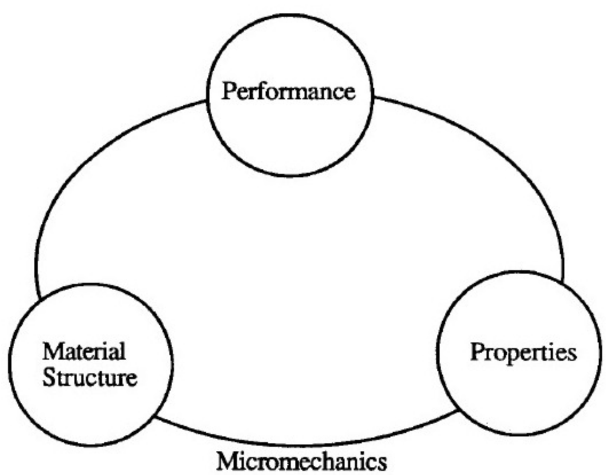


**Figure 2.2 The Performance Driven Design Approach (PDDA)**

This proposed concept excludes the processing aspect for the sake of simplicity. The performance aspect of a structural component can be characterized as deflection control, light weight, seismic resistance, dimensional stability, reliability, and durability. The properties aspect may be defined as moduli, various strength (tensile, compressive, flexural, shear, etc), ductility, toughness, notch sensitivity, density, permeability, coefficient of expansion, and impact, temperature, fatigue and wear resistant properties. The material structure commonly includes the fiber, matrix, and interface. The idea of

PDDA is actually quite simple and normally done. The material chosen should meet the expected structural demand specified by performance and functionalities requirements. In fact, it has been rare to consider a step further approach that is the fiber, matrix, and interfaces are tailored to optimize the needed properties.
The recent increasing availability of a wide range of fiber, cement based matrixes can significantly vary the properties of an FRCC due to a different combinations of fibers, matrices and interfaces. Strain capacity for example can vary by two orders of magnitude. Therefore it is quiet reasonable to tailor the fiber, matrix and interface properties for required composite properties and specified structural performance.
What commonly occur, direct linkages between structural performance and material structures are almost non-existent. This thing is resulting two obstacles namely the improper and limited use of FRCC in structures, and the slow development of advanced FRCCs.
Here, we find that PDDA plays an important role to ensure a direct link between the material composition and the structural performance. Identification of structural performance which can benefit from the special properties of FRCCs should be carried out, and these properties should be related to the microstructures of the FRCC. This approach offers specific guidelines for specific RFCC engineering to meet the specific performance requirements in a specific structure.
To successfully utilize PDDA of FRCC, it will be necessary to clarify the properties associated with the desired structural performance and micromechanical models must be developed to relate such properties to the material microstructures.
An excellent platform has been set by the work of Shah 1990 [13], from which the successful development of FRCCs based on PDDA can be established.

## 2.4 Integrated structures and materials design (ISMD)

Research in materials and structural engineering are frequently carried out separately, meanwhile the significant advances have been made in concrete materials and in concrete structures. This separate way of thinking can lead to opportunity loss in major leaps in structural performance and misleading research emphasis in materials development. Integrated Structures and Materials Design (ISMD) Concept is expected to be an important platform for collaborations between structural engineers and materials engineers, leading to innovative structural and materials designs. The common practices of adding fibers by trial-and-error and then testing for structural element response will not be an efficient approach to materials design, or for achieving deliberate levels of structural performance.
A Performance Based Design Concept (PBDC) adopted by structural design community offer a significant chance for innovative use of materials that in the end lead to the synergism with the Performance Driven Design approach (PDDA) proposed for materials engineering [7]. Integrated Structures and Materials Design (ISMD) scheme is depicted in figure 2.3.

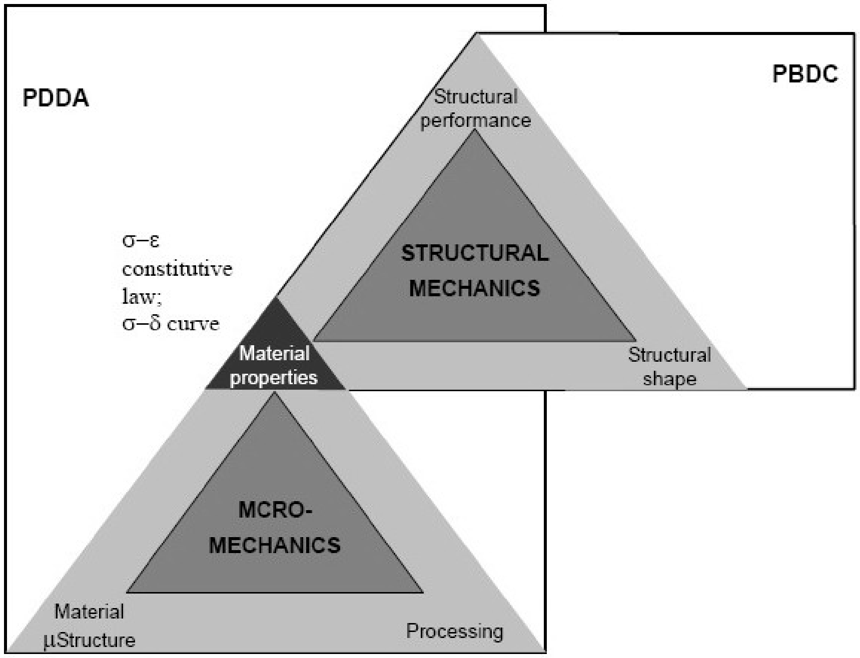


**Figure 2.3 Integrated Structures and Materials Design (ISMD) Concept**

In the upper triangle, structural mechanics relates materials properties and structural shape to structural performance. The Performance Based Design Concept (PBDC) suggests the selection of suitable material properties and structural shape to meet structural performance.
Conceptually, designing for structural performance involves the optimal selection of material and structural shape. This is the typical regime of structural engineering. Traditionally, the menu of construction materials that can be selected for structural applications are rather limited (steel or concrete), so that emphasis is usually placed on designing for the optimum shape given the structural performance requirements. When dealing with mechanical behavior, structural mechanics provides a link between structural shape, materials performance and structural performance.

In the lower triangle, micromechanics relates materials microstructures (which affects and is affected by material processing) to material properties.
In the world of materials engineering, raw ingredients are shaped into a composite through processing. Traditionally, raw ingredient selection is based on empiricism. In recent years, as knowledge of the impact the various phases in a composite have upon macroscopic properties increases, composite materials with specific desirable properties have been systematically designed. A particularly useful set of analytic tools for fiber reinforced cementitious composite design is micromechanics, which quantifies the mechanical interaction between fiber, matrix and fiber/matrix interface and relates this interaction to composite material properties. Micromechanics in this form can be considered analogous to structural mechanics where the fiber, matrix and interface serve as loading-carrying ‘members’, and the composite is regarded as the structural system. Naturally, the length scales are much smaller, and some mechanical or physical phenomena are unique to composite materials.

Micromechanics can be a powerful tool to deliberately tailor the composite ingredients, such as fiber dimensions and surface coatings, along with sand particle amount and size. In addition, knowledge of material processing and its effect on both fresh and hardened properties aids in composite design. Again, while not visible to the eye, this body of knowledge on micromechanics and processing allows systematic development of composites with properties not reachable heretofore. The world of materials engineering, with composite property as the target, is depicted as the lower triangle in Fig. 2.3.

## 2.5 The obstacles and notable mind-frame shift in Implementing ISMD

It is clear from the above discussion and from Fig. 1 that the common link between structural engineering and materials engineering is composite properties. As pointed out previously, performance based design of structures provides flexibility and incentive to deliberately select composite materials with properties that efficiently meet the structural performance target. In turn, modern materials engineering provides the tools for intentionally tailoring material ingredients for desired composite properties. Thus, the integration of structural and materials design is a natural joining of these technical fields. In other engineering fields such as aerospace engineering, such integration has already been in practice for some time. In the discipline of civil engineering, this tighter integration can bring about innovative structural systems unattainable if chasms between the structural engineering and materials engineering fields remain. In most universities, structural engineering and materials engineering are two sub-disciplines within civil engineering. Students in one sub-discipline may lack exposure to the other sub-discipline in their education. This trend unfortunately perpetuates the separation of the two fields as these students continue on as practicing structural or construction materials engineers. In this light, ISMDis not only a collaborative research platform, but also serves as an integrated education platform for future generations of engineers.

Although the concept of integrated structures and materials design is appealing, its implementation faces obstacles requiring attention from both the structural engineering and the materials engineering communities. A shift in mind-frame is needed. The list below is not intended to be exhaustive, but is considered fundamental:

First, material properties characterization should be carried out in such a way that the resulting information can be captured as parameters in constitutive models usable in structural analyses. While this may appear obvious, current standard material tests such as ASTM C1018 which measures toughness based on flexural beams, are of limited use for structural design. It is known that such test results depend on beam height, and are meant to serve only as indices for comparing the relative energy absorption of different fiber mixes.

The second one, structural performance should be translated into demands on composite material properties, and not on specific fiber types. This recognizes that it is the composite properties that govern the structural performance, and not the fiber type. It is understood that fiber type plays an important role in composite properties, but fiber type is only one of many ingredient parameters that govern composite properties. In other words, a specific fiber may give better or worse composite property depending on the interface characteristics and matrix composition.

Last but not least, for ISMD to be successful, materials engineers need to view structural performance as the ultimate goal if materials engineering is to maximize its potential impact on the future practice of civil engineering. Structural engineers need to recognize that increasingly, (beyond dimensioning, and reinforcement type and detailing) concrete materials properties are readily designable, and that in many instances the global performance of a structure can be strongly governed by properties other than compressive strength of concrete materials.

Along these lines, the upper triangle in Fig. 2.3 needs to embrace the lower triangle as an additional degree of freedom of structural design (beyond dimensioning, reinforcement detailing, and choice of concrete compressive strength), while the lower triangle needs to reach upward and embrace structural performance as the ultimate material design objective. These expanded mind-frames support meaningful interactions and collaboration between the two allied communities necessary for the common good of next-generation infrastructure systems which are safe, durable, and sustainable [11].

## 2.6 Micromechanical model

Combining the fracture mechanics and deformation mechanisms, we obtain so called Micromechanical models that make micro-parameter tailoring, which is able to control the failure mode, the tensile strength and the ultimate tensile strain of the composite, possible to be conducted.
Micromechanics models have been proven to be very effective in high performance and cost effective cement-based composites development [14-18].
There are three types of fracture behavior upon first cracking of displacement control uni-axial tensile cementitious materials, namely brittle, quasi-brittle, and strain hardening failure (see Fig. 2.4).

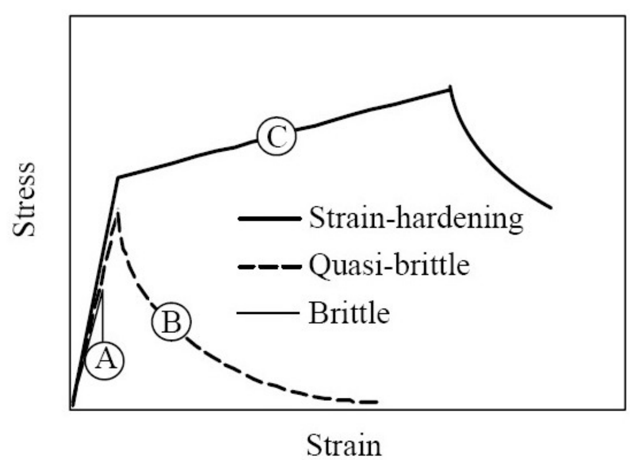


**Figure 2.4 Tensile Failures Modes in Cementitious Materials**

Brittle failure, possibly observed in hardened cement paste material, is described by a linear stress-strain curve (Curve A) accompanied by a sudden drop or complete loss of tensile stress upon first cracking with an ultimate tensile strain in the order of 0.01 %. Quasi brittle behavior, possibly examined in concrete and most fiber reinforced cements and concretes, shows a linear stress-strain curve (Curve B) followed by a gradual decay of tensile stress (softening tail/strain softening) after first cracking, due to the bridging action of aggregates, cement ligaments, and/or fibers. The magnitude of quasi-brittle materials ultimate tensile strain is similar to that from brittle-materials. Strain-hardening is a phenomenon when a material able to sustain increasing level of loading under uni-axial tension after first cracking while undergoing large deformation/ tensile straining (Curve C). The ultimate strain value, at the peak tensile load, of strain-hardening materials can be orders of magnitude higher than that of brittle or quasi-brittle material [18, 8]. A material that shows a strain-hardening behavior with multiple micro-cracking prior to failure develops enhanced ductility. Steady state cracking criterion and first-crack stress criterion are two requirements that should be fulfilled in order to gain strain-hardening behavior. Before describing these two criteria, it is better to firstly explain the composite bridging law [19].

### 2.6.1 Fiber bridging law

Fiber bridging law, also known as the σ(δ) relation, is the relation between stress (σ) transmitted across a crack and crack opening displacement (δ). Stress is transmitted through aggregates and/or fibers, and as a crack open up, transmitted stress increases (called hardening bridging law) or decreases (called softening bridging law). The bridging law is a fundamental material parameter which governs hardening or softening behavior in tension, compression, or flexure [17,8,20-21]. The typical fiber bridging curve can be seen in the following figure. The parameters in the curve will be explained in the next chapter.

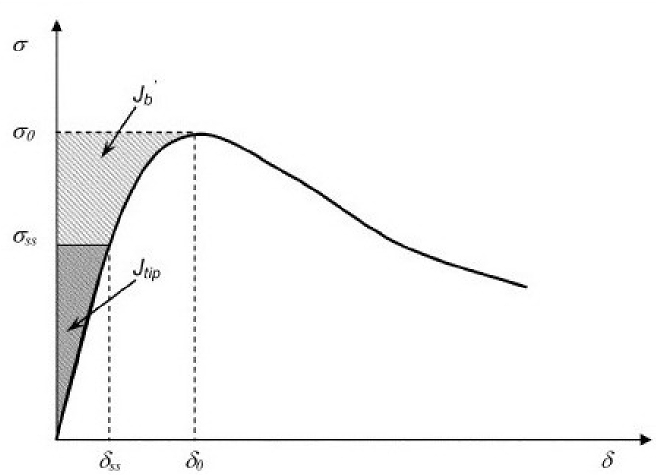


**Figure 2.5 Typical σ(δ) curve for strain-hardening composite**

The significant role of σ(δ) relationship is to provide a link between material micostructure (micro-scale) – fiber, matrix and interface, and the composite ductility (macro-scale) – strain-hardening behavior (see fig. 2.6).

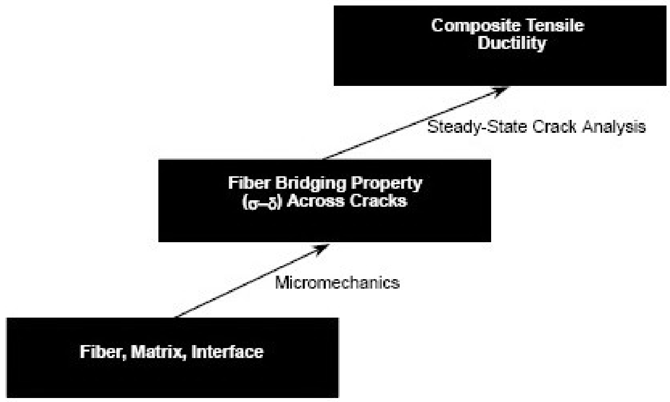


**Figure 2.6 The linkages between materials constituents, crack bridging property and composite tensile ductility**

This means that controlling σ(δ) curve by means of material microstructure tailoring is significant in successfully designing required material properties in general and tensile properties, i.e. tensile strain capacity and ultimate tensile strength, and steady-state crack width in particular. Tensile properties are important to the structural safety at ultimate limit state meanwhile the steady-state crack width is crucial for the structural long-term durability.

## 2.6.2 Strain hardening behavior criteria

The pseudo-strain hardening behavior in ECC is a result of sequential development of matrix multiple cracking. A fundamental requirement for this multiple cracking behavior is that the steady-state cracking occurs under tension, i.e. a flat crack can form after initiating from a defect site and extends indefinitely through the matrix [22]. In this condition, the ambient loading and the crack opening remain constant and bridging fiber sustain and pass the load without rupturing and diminishing. Further loading initiates another microcrack from another defect site and subsequent flat crack propagation. Repeated formation of such steady-state cracks results in multiple cracking and strain-hardening.

The condition for steady-state flat crack propagation was analyzed by Marshall and Cox (1998) using J-integral method. When fiber-bridging behavior is characterized by the σ(δ) relation, the condition can be expressed in the following form:

$$J_{tip} \le \sigma_0\delta_0 - \int_0^{\delta_0} \sigma(\delta)d\delta \equiv J_b^{'} \tag{1}$$

The steady crack criterion will assure the presence of multiple cracking if the complementary energy $J_b^{'}$ is equal to, or greater than the matrix crack tip toughness $J_{tip}$ (Eq. 1). Equation (1) expresses the energy balance (energy supplied by external work and energy consumed by material break-down at the crack tip and subsequently opening of the springs near the crack tip) per unit crack advance during steady-state propagation.

Figure 1 schematically illustrates such energy balance concept, where $J_b^{'}$ and $J_{tip}$ are represented by the hatched and shaded area respectively.

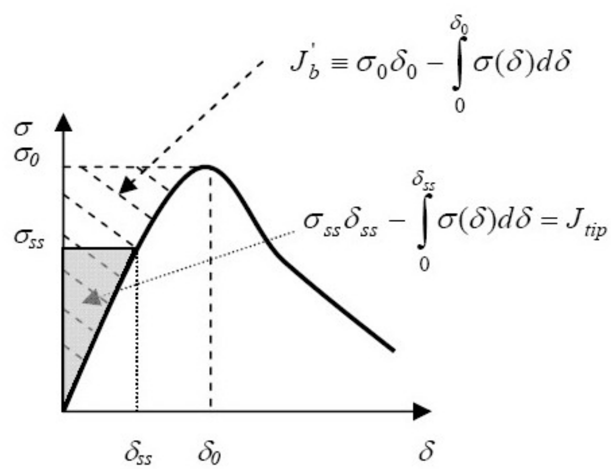


**Figure 2.7 σ(δ) curve for tensile strain-hardening composite.**

The steady state crack stress $\sigma_{ss}$ can be expressed as equation (2).

$$\sigma_{ss}\delta_{ss} - \int_0^{\delta_{ss}} \sigma(\delta)d\delta = J_{tip} \tag{2}$$

Jtip approaches the matrix toughness $K_m^2/E_m$ at small fiber content, where $K_m$ is the matrix fracture toughness and $E_m$ is the matrix Young's modulus. It is appropriate for ECC because less than 3% fiber by volume is used. Thus, equation (1) can be expressed as following.

$$\frac{K_m^{\ 2}}{E_m} \le \sigma_0\delta_0 - \int_0^{\delta_0} \sigma(\delta)d\delta \equiv J_b^{'} \tag{3}$$

It is clear from Eq. (2) that the successful design of an ECC requires the tailoring of matrix, fiber, and interface properties. Specifically, the fiber and interface properties control the shape of the σ(δ) curve and are therefore the dominant factors governing $J_b^{'}$. The composite design for strain-hardening requires the tailoring of the fiber/matrix interface to maximize the value of $J_b^{'}$ [6]

The shape of the σ(δ) curve and especially the rising branch associated with $J_b^{'}$ shown in Fig. 1 is related to a number of fiber/matrix interaction mechanisms. In the simplest case when fibers and matrix are in frictional contact only, the slope of the rising branch of the σ(δ) curve, or the stiffness of the bridges, is mainly governed by the fiber content $V_f$, the fiber diameter $d_f$, fiber length $L_f$ and stiffness $E_f$, and the interface frictional bond $\tau_0$. In the case when chemical bond $G_d$ is present, the starting point of the σ(δ) is not at the origin of the plot but is shifted upwards. This reflects the need of a certain amount of load on the fibers and interface before the interfacial chemical bond can be broken. Dedonding is needed to allow for deformation of the debonded fiber segment to produce crack opening d. Thus, the presence of $G_d$ typically diminishes the complementary energy $J_b^{'}$.

The peak value of the $\sigma(\delta)$ curve is mainly governed by $V_f$, $d_f$, $L_f$, $\tau_0$ in the case of simple friction pullout. An analytic expression of $\sigma_0$ can be found in Li [20]. In the presence of $G_d$, the higher load on the fiber can lead to fiber rupture. Thus, for given fiber strength $\sigma_f$, the complementary energy $J_b^{'}$ again decreases with $G_d$.

Information on fiber tailoring can be found in Wu [23]. An initial study on matrix tailoring using fine sand was reported in Li, Wang, and Wu [24]. The tailoring of the fiber/matrix interface to create the extremely ductile PVA-ECC composite can be found in Li, Wu, Wang, Ogawa, and Saito [6].

Prior to flat crack propagation, it is necessary for a microcrack to initiate (from a defect site) at a load level below the fiber-bridging capacity. This consideration translates into another condition for strain-hardening: that the matrix tensile cracking strength $\sigma_c$ must not exceed the maximum fiber-bridging strength $\sigma_0$ [22].

$$\sigma_c < \sigma_0 \tag{4}$$

Where $\sigma_c$ is determined by the pre-existing flaw size and the matrix fracture toughness Km. While the energy criterion (Eq. 1) governs the crack propagation mode, the strength-based criterion represented by equation (2) governs the initiation of cracks. Satisfaction of both equation (1) and (2) is necessary to achieve ECC tensile strain-hardening behavior; otherwise, relatively poor tensile strain-capacity or even normal tension-softening FRC behavior results.

As can be seen, both criteria are related to fiber-bridging constitutive law. It determines the complementary energy $J_b^{'}$ in equation (1) as well as the maximum bridging strength $\sigma_0$ in equation (2). Therefore, the $\sigma(\delta)$ relationship critically controls the tensile strain-hardening behavior of ECC materials.

## 2.7 Properties of cement based fiber composite material constituents

A major challenge to the research community is to develop a new type of fiber reinforced concrete (FRC) which has the following favorable characteristic:

a. Flexible processing, i.e. can be used in pre-cast or cast-in-place applications and no requirement of very special processing machinery.
b. Short fibers of moderate volume fraction to maintain flexible processing, reduce cost and weight.
c. Isotropic properties, i.e. no weak planes under multi-axial loading conditions in bulk structures.
d. High performance, i.e. leading to significant improvements in strength, ductility, fracture toughness, and exhibit pseudo strain-hardening.

Conventionally, research has focused on studying the property dependence of FRC on one or two parameters at a time, typically the fiber volume fraction, or fiber length. However, it is now well-known that the composite properties depend on three groups of constituent properties – the fiber, matrix, and interface properties (table 2.2).

**Table 2.2 Cement based fiber composite material constituents and their properties**

| **Constituents** | **Properties** |
|---|---|
| Fiber | Elastic modulus, tensile strength, length, diameter, volume fraction. |
| Matrix | Fracture toughness, elastic modulus, initial flaw size |
| Interface | Bond properties, snubbing coefficient |

The importance of this is the recognition that fiber volume fraction, for example, is only one of 10 other micromechanical properties of fiber-matrix system under our control. It is not enough to understand the individual influence of each parameter on composite properties, which can be (at least in principle) established empirically. Composite optimization requires that the combined influence of all relevant parameters on composite properties be known. Composite optimization can lead to a composite with excellent performance, of an ideal FRC described above, with only moderate fiber volume fraction. To establish the combined influence of the constituent parameters on composite properties, it is necessary to develop a fundamental understanding of the micro-mechanisms which govern a given material property. (As a simple example, it is well-known that the unstable propagation of a material defect in the form of a pre-existing crack governs the tensile strength of a brittle solid). Based on this understanding, it will be possible to identify the material microstructure and associated properties which control composite behavior. (The above example will lead to the defect size and intrinsic fracture toughness as micro-parameters governing the brittle material strength). Hence micromechanics serves to establish the link between material constituents and composite properties. The resulting information can be used to advantage for composite design. When fully developed, micromechanics can also be utilized as a tool for material property tailoring. The use of micromechanics based approach to engineering an FRC resulting a new class of materials called Engineered Cementitious Composites (ECC) [18].

# Chapter 3 Existing Analytical and Experimental Results

This chapter presents the experimental and analytical results have already been done by Prof. Victor C. Li who developed ECC at University of Michigan. The results consist of single fiber test, uni-axial tensile test, and four point bending test.

## 3.1 Material properties

As mentioned before, the composite performance is described by 11 (eleven) micro-mechanical properties of the fiber-matrix system [14]:

a. Fiber parameters: fiber length ($L_f$), fiber diameter ($d_f$), fiber stiffness ($E_f$), fiber strength ($\sigma_f$), and fiber volume fraction ($V_f$).
b. Matrix parameters: matrix stiffness ($E_m$), matrix fracture toughness ($K_m$), and initial flaw size (c).
c. Fiber-matrix interaction parameters: interfacial frictional bond ($\tau_0$), interfacial chemical bond ($G_d$), and snubbing coefficient (f).

Km is measured from four point bending tests. The fiber matrix interface properties are measured from single fiber pull-out tests: a fiber with a controlled embedment length is pulled out from a block of matrix while load vs displacement relation is recorded [6]

## 3.2 Single fiber tensile test

Single fiber pull-out problem is a complicated solid mechanics problem. An analytical fiber-bridging model is currently in progress and experimentally verified. The model is improved by including several mechanisms of fiber-matrix interactions in order to accurately predict the $\sigma(\delta)$ curve in general and improve accuracy of crack opening prediction in particular. Two way fiber pull-out behavior is considered in the model which includes both chemical bond ($G_d$) and slip hardening coefficient ($\beta$). A complete analytical formulation can be found in Lin, Kanda, and Li [14].
Below (Fig 4) is the comparison curve between test result and analytical prediction model for single fiber pull-out test taken from [14].

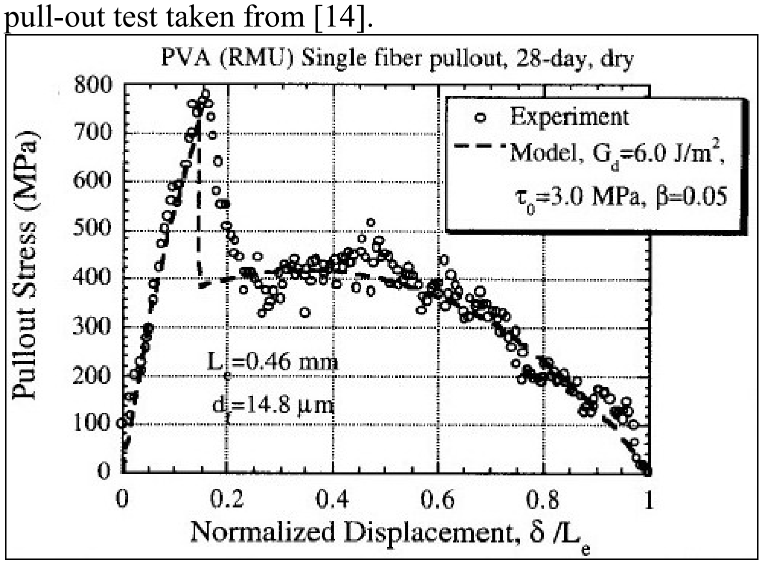


**Figure 3.1 Single fiber pull-out curve of a PVA fiber: Test result vs. model prediction [14]**

As can be seen from Fig. 3.1, there are three stages associated with the load displacement curve: initial elastic stretching of the fiber free length (the portion not embedded), followed by debonding stage, which is simulated in the present model by a mode-II tunneling crack advance with non-zero crack-tip fracture toughness. The debonding stage continues until reaching the maximum load and a distinct load drop occurs. This load drop is an indication of chemical bonding because it would not appear if the interface is frictionally bonded only. Physically, the load drop represents the transition from both chemical bond and frictional bond controlled debonding stage to the pull-out stage with frictional bond only

After complete debonding of the interface, chemical bond does not exist but frictional bond could effectively increase due to fibrillation of fiber surface sliding against surrounding matrix. A concave upward portion of the curve indicates this so called slip hardening behavior, which has been investigated in [25, 26]

## 3.3 Uni-axial tensile test

ECC is a cement based composite and usually reinforced with short (6-12 mm), randomly distributed small diameter (10-100 μm) micro-fiber. The construction of fiber bridging constitutive law starts from modeling a single fiber pull-out behavior against the surrounding matrix. The σ(δ) relationship can then be obtained by averaging the contribution from fibers with different embedment length and orientation across the crack plane. So far, the mechanisms incorporated in the model namely: two-way fiber pull-out behavior, matrix micro-spalling, average-modeling of fiber randomness, and cook-gordon effect. Due to absence of coarse aggregate in ECC mix design, aggregate bridging is not considered [27].

The comparison between model prediction and experiment results for uni-axial tensile test of specimen with fibers taken from [27] can be seen as following.

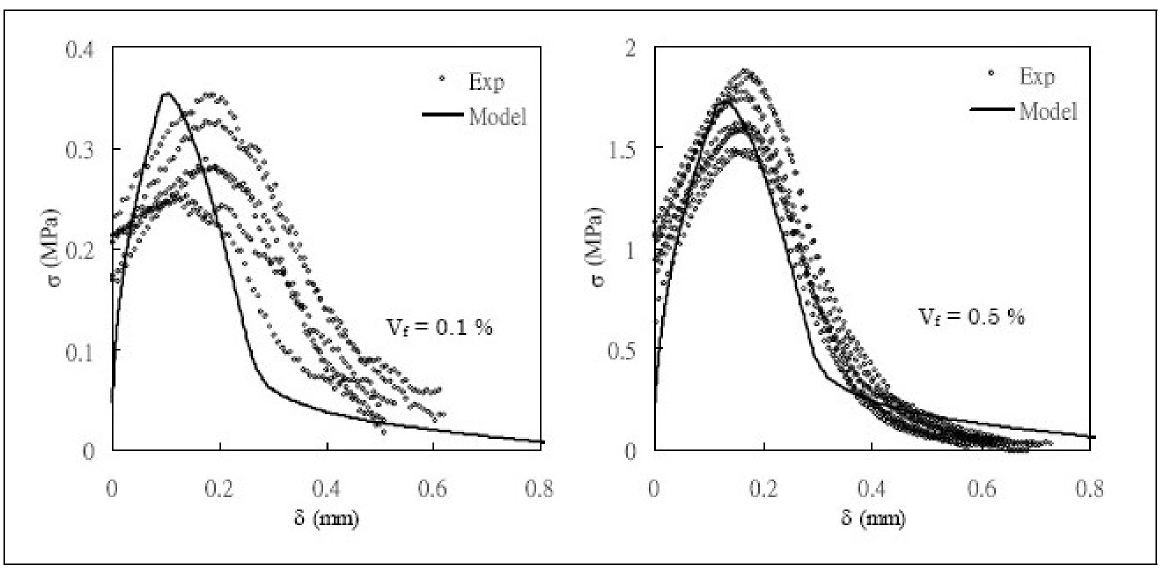


**Figure 3.2 Comparison of σ(δ) curves obtained from uni-axial tensile tests of notched specimens and from model predictions of PVA-ECC for (a) $V_f$ = 0.1 vol.% and (b) $V_f$ = 0.5 vol.%**

The analytical σ(δ) curve can be calculated as long as all micromechanics parameters are determined. 2-D random fiber distribution was assumed in calculating the fiber-bridging model for comparison with experimental σ(δ) curves measured from coupon specimens. Because the thickness of the coupon specimen is small (13 mm) when compared with fiber length (12 mm), fiber is most likely distributed in a 2-D randomness manner. Fig. 3.2 shows the predicted fiber bridging constitutive law (solid line) for M45 (see table 3.1) with Vf = 0.5 and 0.1 vol.%, respectively. In calculating these two curves, all micromechanics parameters for model input are listed in table 3 and 4. Post-cracking σ(δ) curve (hollow circular dots) measured experimentally are also plotted together with the model prediction in Fig. 3.2 for comparison purpose. At least 6 uni-axial tensile tests were conducted and reported in Fig. 3.2 for each fiber volume.

The scattered σ(δ) curves obtained from experiments are results of material inhomogeneity, e.g. varying number of bridging fiber across crack plane for the six different specimens. Although the peak bridging stress varies in a wider range, the corresponding crack opening δ remains fairly constant. This is likely a result that with larger number of fibers, a higher load can be reached, but the crack opening will be limited by an effectively stiffer (averaged) fiber spring. This observation is also consistent with the two sets of experimental data of Vf = 0.1 and Vf = 0.5. As can be seen, the predicted σ(δ) curves which represent the mean fiber bridging constitutive law fit well with experimental observations and the validity of this newly developed σ(δ) model is therefore confirmed.

| Vf (vol.%) | Cement ($kg/m^3$) | Fly Ash ($kg/m^3$) | Sand ($kg/m^3$) | Water ($kg/m^3$) | HRWR(1) ($kg/m^3$) | Fiber(2) ($kg/m^3$) | Total ($kg/m^3$) |
|---|---|---|---|---|---|---|---|
| 0.1 | 571 | 685 | 456 | 332 | 6.8 | 1.3 | 2052.1 |
| 0.5 | 571 | 685 | 456 | 332 | 6.8 | 6.5 | 2057.3 |

**Table 3.1 Mix properties of PVA-ECC (M45)**

(1) polycarboxylate-based high range water reducer
(2) PVA fiber

| Fiber parameters | | | | Interface parameters | | | Matrix parameters | | |
|---|---|---|---|---|---|---|---|---|---|
| $d_f$ (μm) | $L_f$ (mm) | $E_f$ (GPa) | $\sigma_{fu}$ (MPa) | f | f' | α (μm) | $E_m$ (MPa) | $\sigma_m$ (MPa) | k |
| 39 | 12 | 22 | 1060 | 0.2 | 0.33 | 78 | 20 | 5 | 500 |

**Table 3.2 Micromechanics parameters used as model input**

| Matrix type | $\tau_0$ (MPa) | Gd ($J/m^2$) | β |
|---|---|---|---|
| 0.1 % vol.% PVA | 1.91 | 1.24 | 0.63 |
| 0.5 % vol.% PVA | 1.58 | 1.13 | 0.60 |

**Table 3.3 Interfacial properties of ECC**

## 3.4 Four point bending test

Another way of obtaining σ(δ) curve is by performing four point bending test which will also give information about the matrix fracture toughness. The following result is taken from experiment done by Li [18].

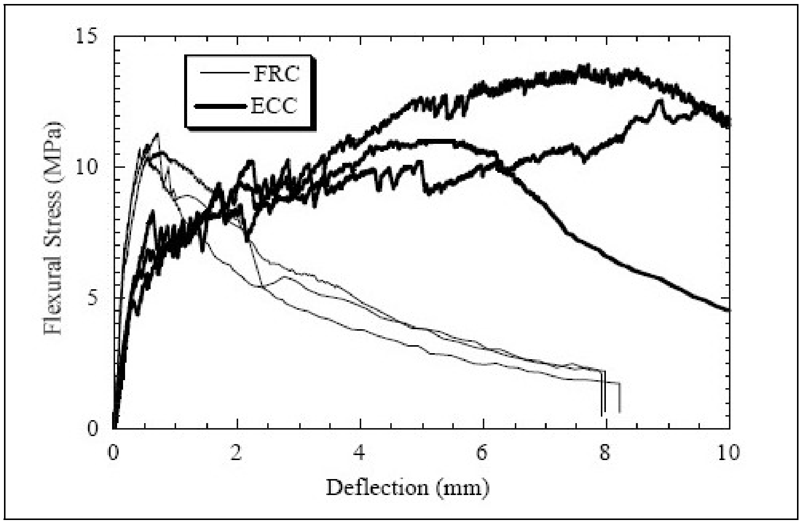

**Fig 3.3 Flexural stress-deflection curve for ECC and FRC**

The experimental set-up is based on ASTM C78-75. The flexural stress-deflection curves of the ECC are shown in Fig. 3.3. For comparison, the stress-deflection curves for a 1% steel FRC are also shown. For the steel FRC, the flexural stress increases rapidly to the peak value and then starts to decay. The average beam deflection at peak stress is about 0.6 mm. For the ECC, however, the flexural stress increases at a slower rate. This increase is accompanied by the development of multiple fine cracks. The average beam deflection at peak stress is about 7.4 mm. The flexural strength (MOR) for the ECC is determined to be 12.5 MPa, compared to 10.9 MPa for the steel FRC. Although toughness index has not been measured for the ECC, it is expected to be much higher than the FRC based on the area under their flexural stress-deflection curves.

The crack pattern of the ECC is distinctly different from plain concrete or normal FRC. The first crack started inside the mid-span at the tensile face, and multiple cracks developed from the first cracking point and spread to the outside of the mid-span. The multiple cracks in the outside of the mid-span were inclined cracks similar to shear cracks in steel reinforced concrete (R/C) beams. As the MOR is approached, one of the cracks inside the mid-span started to open up after a large damage zone had been developed. The through-thickness damage zone can reach an areal dimension of 200 $cm^2$. Fig. 3.4 shows a typical cracking pattern that develops in the beam middle span around the peak load.

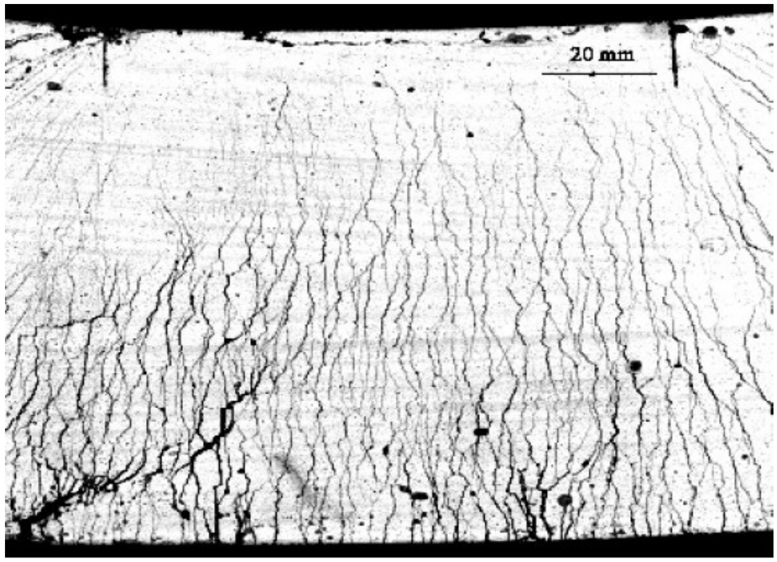


**Fig 3.4 Cracking pattern in ECC beam mid-span around peak load [18]**

For ideally brittle material, the MOR to tensile strength ratio is unity. For quasi-brittle material such as concrete or FRC, this ratio lies between 1 and 3. The upper limit describes the case of a elastic-perfectly plastic material. For the case of ECC, this ratio can be expected to be higher than 3 due to the strain-hardening nature after first crack. This expectation is confirmed by the test results which show that the ratio is equal to 5.0 for the ECC, compared to 2.5 for the FRC.

# Chapter 4 3D Lattice Fracture Analysis

This chapter gives the results of 3D lattice fracture analysis of single fiber test, uni-axial tensile test, and four point bending test. An overview of the model which is used is also explained.

## 4.1 Overview

One may obtain a huge variety of Cement based fiber reinforced materials with their applications or perhaps currently still developed in research laboratories worldwide [28]. Numerous researches have been done under an effort to improve the ductility of concrete materials. It occurs due to the fact that most of the problems in infrastructure deteriorations and failures emerged from crack and brittle behavior of concrete. The current experiment shows that the most effective way of enhancing concrete ductility is by adding fibers [6]. Nowadays, different type of fibers have been used, such as steel, PVA, PE, glass, and even natural fibers. The research advances in this field yield a class of ultra ductile fiber reinforced cementitious composites called ECC (Engineered Cementitious Composites). Occasionally, these materials exhibit an extremely high strain capacity of more than 6% and a distributed crack pattern with fine cracks under imposed deformation loading. These material behaviors are achieved through microstructures tailoring including matrix, fiber, and interface parameter [7].

Basically, all these parameters can be obtained through laboratory experiments but due to quite time consuming, a 3D numerical model is used [29].

## 4.2 3-D lattice model for fiber-matrix composite

The model described in this writing is based on [29]. See Fig.1 to see 2D representation of the real 3D Mesh.

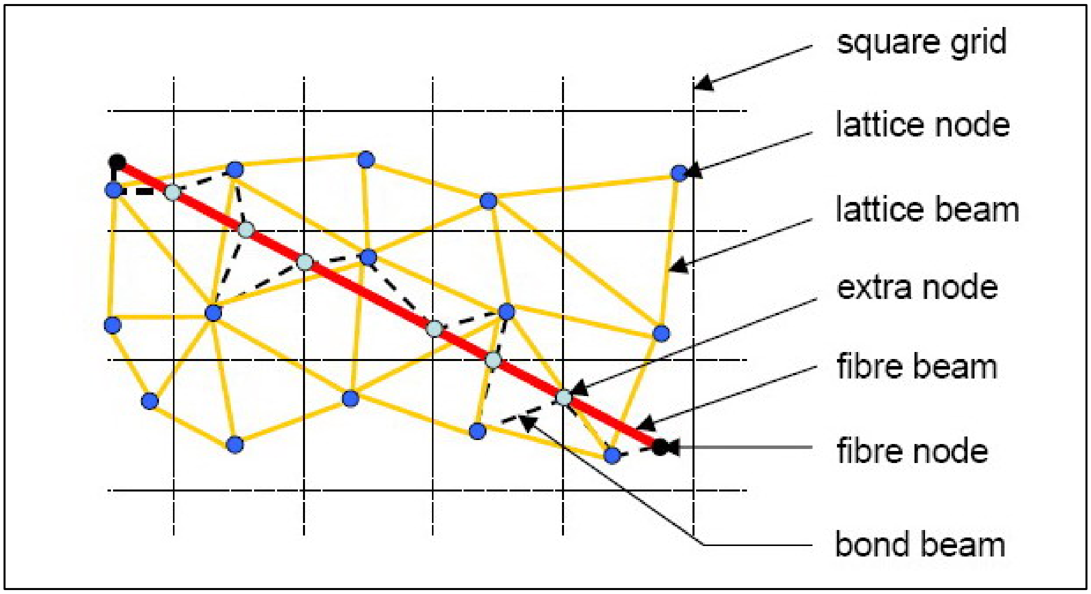


**Figure 4.1 Schematic 2D representation of generation of fiber-lattice**

The 3D model consists of the following items:

a. Square Grid
The grid is used to limit the domain of each random lattice node in the 3D space. This square grid actually has cubical shape for 3D model.

b. Lattice Node
A lattice Node is generated randomly within each square grid. It takes certain coordinate in 3D coordinate system.

c. Lattice Beam
The lattice nodes which are closest each other are connected by Lattice beam elements. These Beam elements represent the cement matrix.

d. Fiber Node
Fiber Nodes will be randomly chosen in the volume after fiber elements are generated.

e. Fiber Beam
The number of the fiber, placed in certain volume, is calculated based on the length, diameter, and volume percentage of fibers.

f. Extra Node
Extra Nodes are generated at each location where the fiber crosses the square grid.

g. Bond Beam
Bond Beam are generated between fiber nodes and the lattice nodes in the neighboring cell.

All the elements in the network are beam elements (with normal force, shear forces, bending moments and torsion moment), which have a local brittle behaviour. The beam elements fail only in tension (except for the interface elements, which can also fail in compression) when the stress of the element exceeds its strength. For the fracture criteria only the normal force is taken into account to determine the stress in the beams.

## 4.3 Single fiber tensile test

This section will explain the result of fiber tensile test based on Prabowo [30]. All lattice fracture simulations have been done by using GLAK (Generalized Lattice Analysis Kernel) developed by Qian [31].
Before doing the tensile test simulation it is quite important to set the diameter of the cement matrix such that the Matrix Elastic Modulus is similar to Lattice model Elastic Modulus. It is done in order to guarantee that the model is the same as expected from the input value. It is found that the matrix radius should be 0.5 mm to achieved 30 GPa matrix Elastic modulus. The simulation also shows that the Elastic modulus is independent of specimen size. On the other hand, Elastic modulus is influenced by the changing of matrix radius.

In this simulation, specimen 5x5x30 is used with 10 mm fiber embedment length.
The Matrix and fiber properties are kept constant as following:

| | **Radius (mm)** | **E (GPa)** | **ft (Mpa)** | **fc (Mpa)** |
|---|---|---|---|---|
| **Matrix** | 0.5 | 30 | 5 | - |
| **Fibre** | 0.3 | 40 | 700 | - |

**Table 4.1 Matrix and Fiber Properties**

The interface radius is varied by 0.1 mm, 0.5 mm, and 1.0 mm. The elastic modulus is differed by 5, 10 and 15 GPa, meanwhile the tensile strength are 100, 300 and 500 GPa and compressive strength are -300, -600 and -900 respectively.
The matrix-fiber system properties that is considered resulting the ductile fiber-reinforced materials can be seen in the following table.

| | Radius (mm) | E (GPa) | ν, Poisson's ratio | G (MPa) | ft (MPa) | fc (MPa) |
|---|---|---|---|---|---|---|
| Matrix | 0.5 | 30 | 0.2 | 12500 | 5 | - |
| Interface | 0.1 | 5 | 0.333 | 1875 | 100 | -300 |
| Fiber | 0.022 | 41.1 | 0.35 | 15222 | 1640 | - |

**Table 4.2 Matrix-Fiber System Properties**

## 4.4 Uni-axial tensile test

The simulation is carried out by using 8x5x30 specimen with fiber length 8 mm, and fiber volume fraction 1% and 2%. The matrix-fiber system properties from the single fiber pull-out test are used due to their good results.

| | Radius (mm) | E (GPa) | ν, Poisson's ratio | G (MPa) | ft (MPa) | fc (MPa) |
|---|---|---|---|---|---|---|
| Matrix | 0.5 | 30 | 0.2 | 12500 | 5 | - |
| Interface | 0.1 | 5 | 0.333 | 1875 | 100 | -300 |
| Fiber | 0.022 | 41.1 | 0.35 | 15222 | 1640 | - |

**Table 4.3 Matrix-Fiber System Properties**

Matrix properties taken from [30], Fiber properties taken from [32], its poisson's ratio taken from [33], and Interface properties taken from [30].

The general simulation procedure can be summarized as follow:

1. Generate 3D Random Lattice

In this step, the size of the tested specimen is defined. The lattice node and lattice beam for matrix element are generated.

2. Input the properties of the matrix element

The properties of matrix element are assigned in this stage.

3. Generate fiber element

Fiber elements are generated according to fiber volume fraction and fiber length.

4. Add fiber element to 3D Random Lattice

The fibers are introduced to 3D Random lattice system. Extra nodes are generated at each location where the fiber crosses the square grid. Bond beam which represents the interface element are generated between fiber nodes and the lattice nodes in the neighboring cell. The properties for fiber and interface elements are defined.

5. Adding fiber Nodes at boundary

The position of the support and the applied external load are assigned.

6. Make image for initial lattice element

The initial element images are made to check for the desired model.

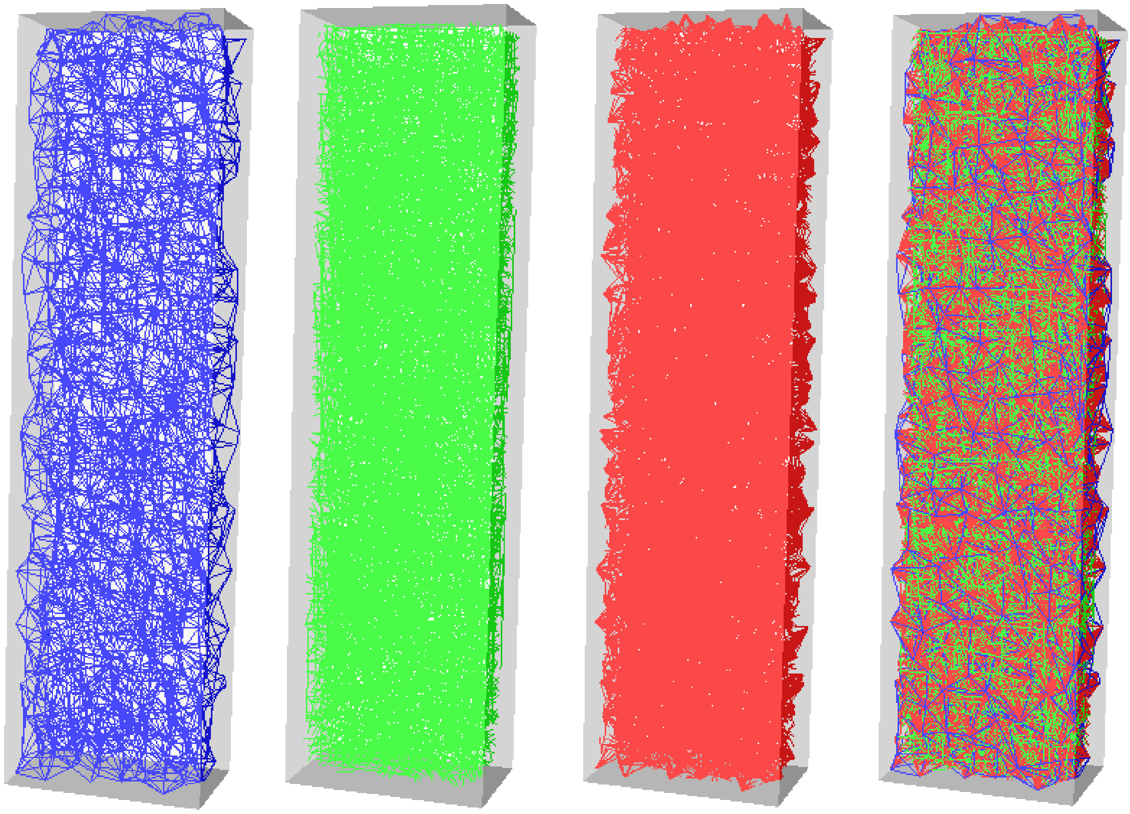

**Figure 4.2 Undamaged Element Images (Matrix, Fiber, Interface, Matrix-Fiber system respectively) for 2% fiber volume fraction**

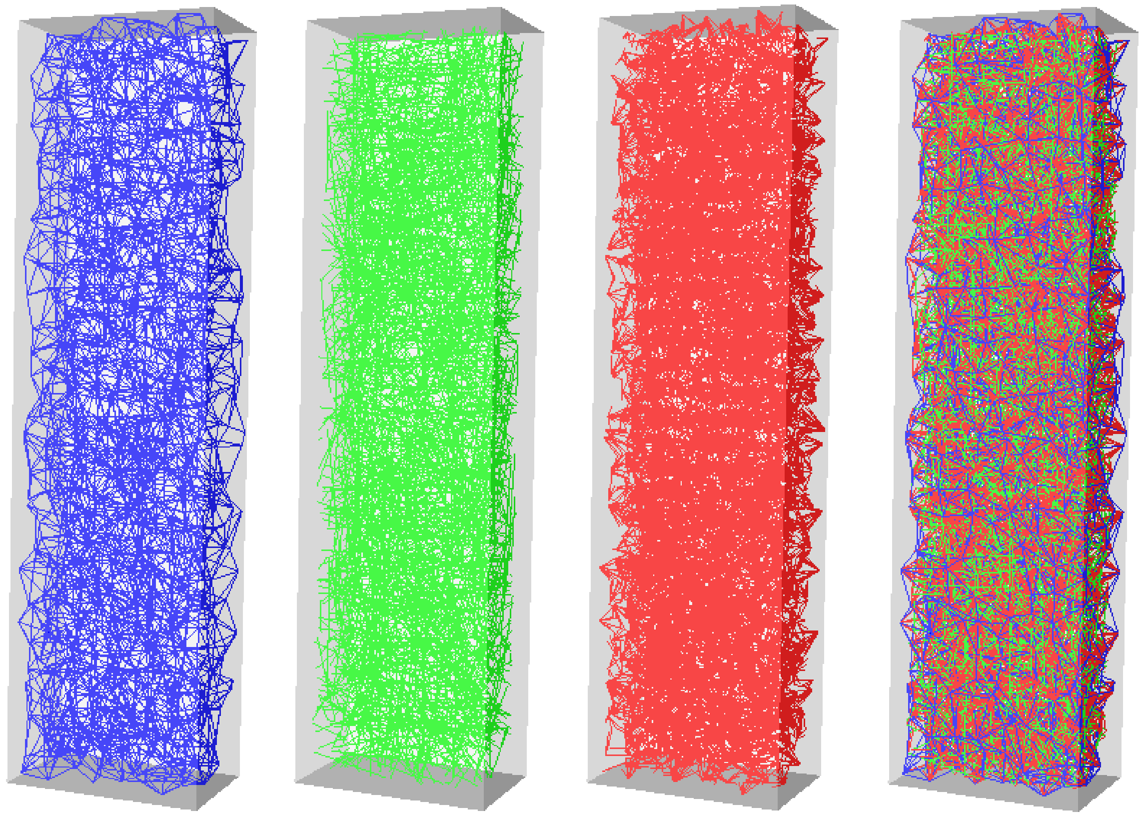

**Figure 4.3 Undamaged Element Images (Matrix, Fiber, Interface, Matrix-Fiber system respectively) for 1% fiber volume fraction**

7. GLAK Simulation

The lattice fracture simulations are done by using GLAK (Generalized Lattice Analysis Kernel). The procedure sequence in this step include performing a linear elastic analysis, calculating stresses in all the beams, removing one beam following strength criteria, and relaxing the displacements and removing next beam.

8. Make uni-axial tensile test graph from simulation results

The graph is plotted from the simulation result and determine the specimen behavior whether it is brittle, quasi-brittle or showing interesting strain-hardening failure.

9. Make image for damaged lattice element

This step is intended to investigate the crack patterns within the specimen which correspond to certain position in load deformation curve.

### 4.4.1 First simulation

The first simulation is done by using 6 (six) combinations. Only the Interface Elastic modulus that is varied and the other parameters are kept constant. The Interface Elastic modulus used are 0.4; 5; 0.1; 10; 20 and 50 GPa for combination 1, 2, 3, 4, 5, and 6 respectively. The fiber volume fractions used are 1% and 2%. The simulation result can be seen as following.

**Combo 1 (2% Fibers)**

| | Radius (mm) | E (GPa) | ν, Poisson's ratio | G (MPa) | ft (MPa) | fc (MPa) |
|---|---|---|---|---|---|---|
| Matrix | 0.5 | 30 | 0.2 | 12500 | 5 | - |
| Interface | 0.1 | 0.4 | 0.333 | 150 | 100 | -300 |
| Fiber | 0.022 | 41.1 | 0.35 | 15222 | 1640 | - |

**Table 4.4 Matrix-Fiber System Properties**

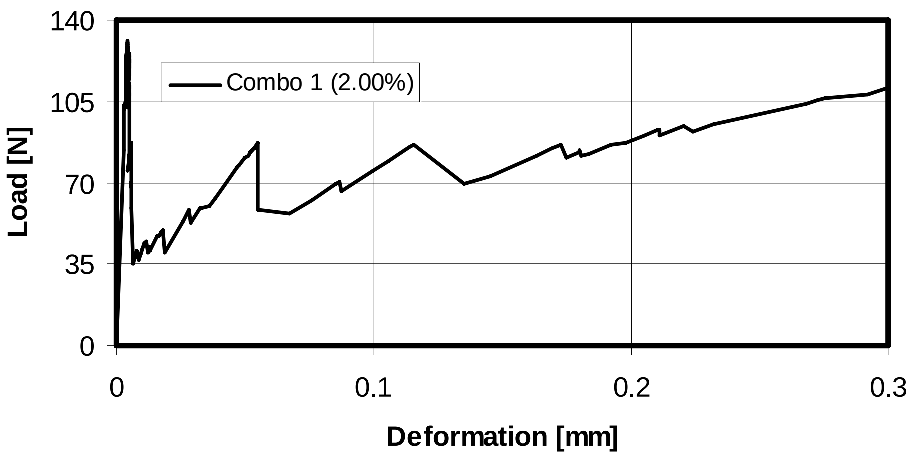


**Figure 4.2 Load displacement curve**

**Combo 2 (2% Fibers)**

| | Radius (mm) | E (GPa) | ν, Poisson's ratio | G (MPa) | ft (MPa) | fc (MPa) |
|---|---|---|---|---|---|---|
| Matrix | 0.5 | 30 | 0.2 | 12500 | 5 | - |
| Interface | 0.1 | 5 | 0.333 | 1875 | 100 | -300 |
| Fiber | 0.022 | 41.1 | 0.35 | 15222 | 1640 | - |

**Table 4.5 Matrix-Fiber System Properties**

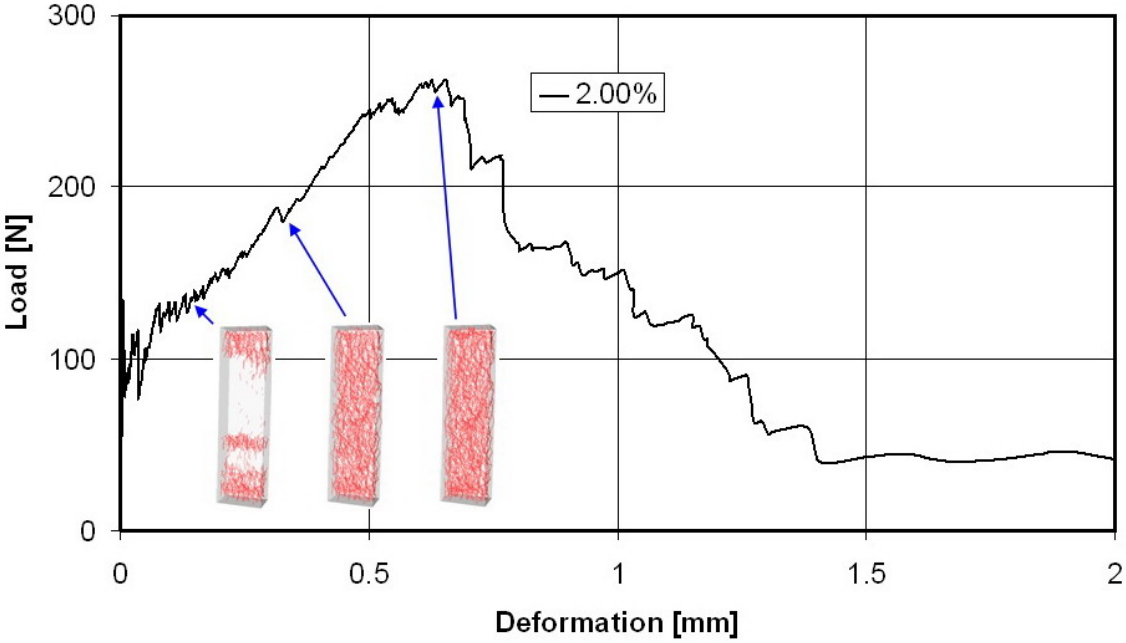


**Figure 4.3 Load displacement curve**

## Combo 2 (1% Fibers)

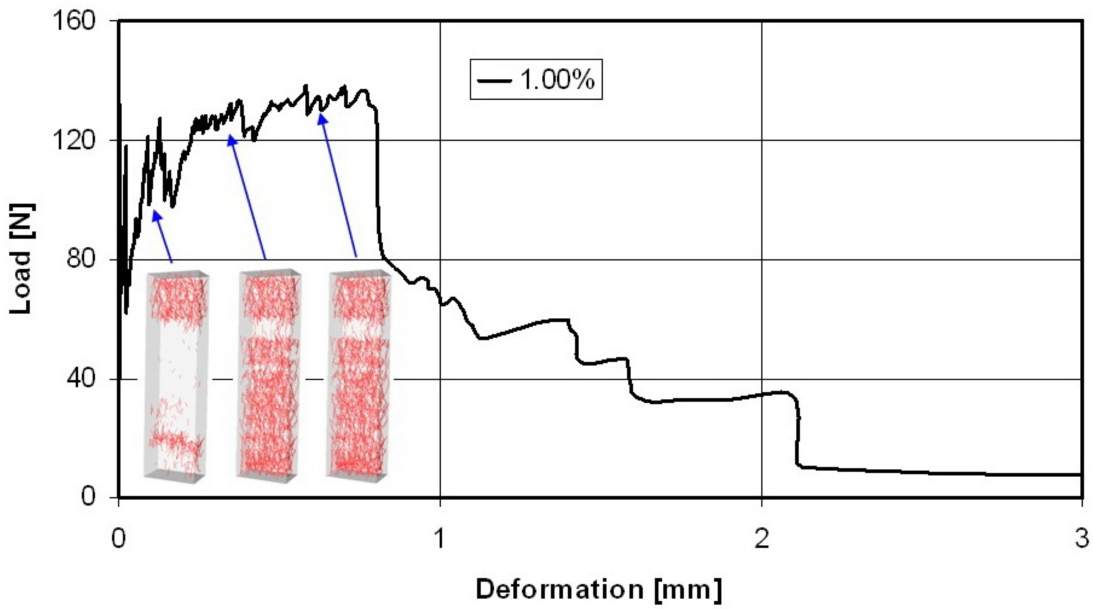


**Figure 4.4 Load displacement curve**

**Combo 3 (2% Fibers)**

| | Radius (mm) | E (GPa) | ν, Poisson's ratio | G (MPa) | ft (MPa) | fc (MPa) |
|---|---|---|---|---|---|---|
| Matrix | 0.5 | 30 | 0.2 | 12500 | 5 | - |
| Interface | 0.1 | 0.1 | 0.333 | 37.5 | 100 | -300 |
| Fiber | 0.022 | 41.1 | 0.35 | 15222 | 1640 | - |

**Table 4.6 Matrix-Fiber System Properties**

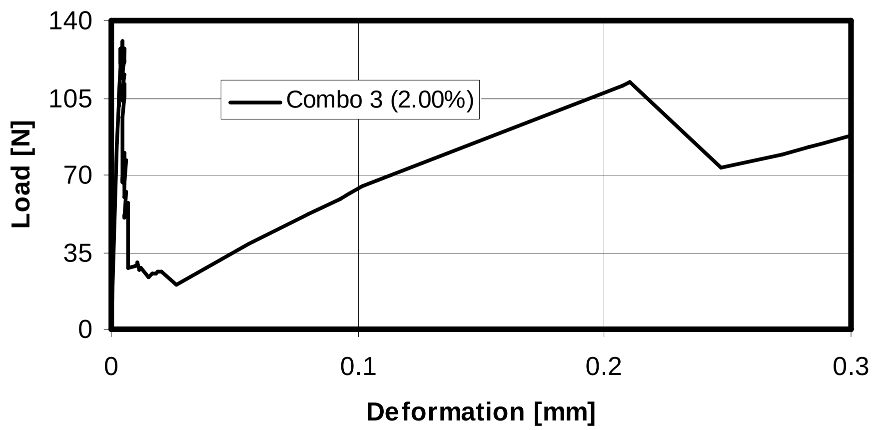


**Figure 4.5 Load displacement curve**

**Combo 4 (2% Fibers)**

| | Radius (mm) | E (GPa) | ν, Poisson's ratio | G (MPa) | ft (MPa) | fc (MPa) |
|---|---|---|---|---|---|---|
| Matrix | 0.5 | 30 | 0.2 | 12500 | 5 | - |
| Interface | 0.1 | 10 | 0.333 | 3750 | 100 | -300 |
| Fiber | 0.022 | 41.1 | 0.35 | 15222 | 1640 | - |

**Table 4.7 Matrix-Fiber System Properties**

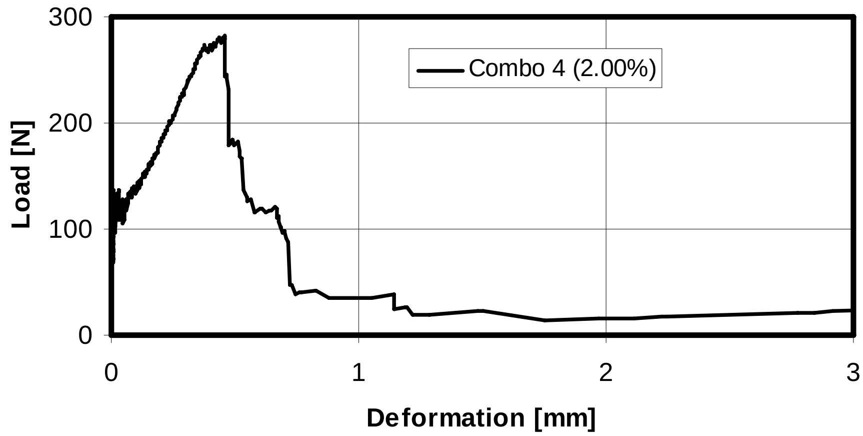


**Figure 4.6 Load displacement curve**

## Combo 4 (1% Fibers)

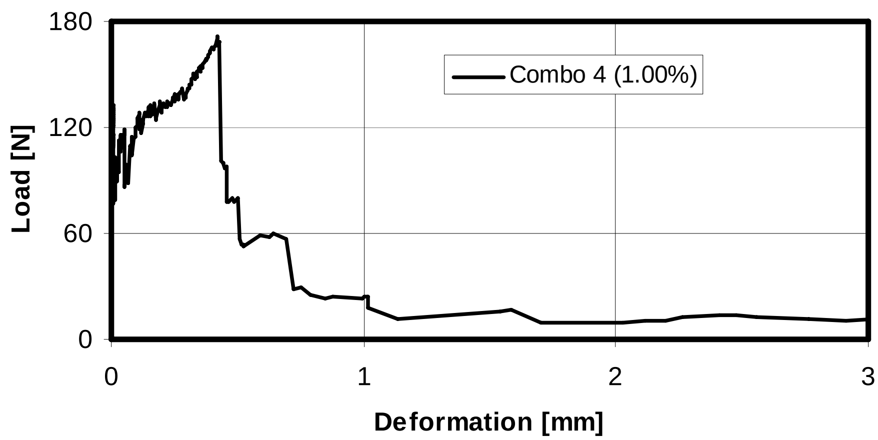


**Figure 4.7 Load displacement curve**

## Combo 5 (2% Fibers)

| | Radius (mm) | E (GPa) | ν, Poisson's ratio | G (MPa) | ft (MPa) | fc (MPa) |
|---|---|---|---|---|---|---|
| Matrix | 0.5 | 30 | 0.2 | 12500 | 5 | - |
| Interface | 0.1 | 20 | 0.333 | 7500 | 100 | -300 |
| Fiber | 0.022 | 41.1 | 0.35 | 15222 | 1640 | - |

**Table 4.8 Matrix-Fiber System Properties**

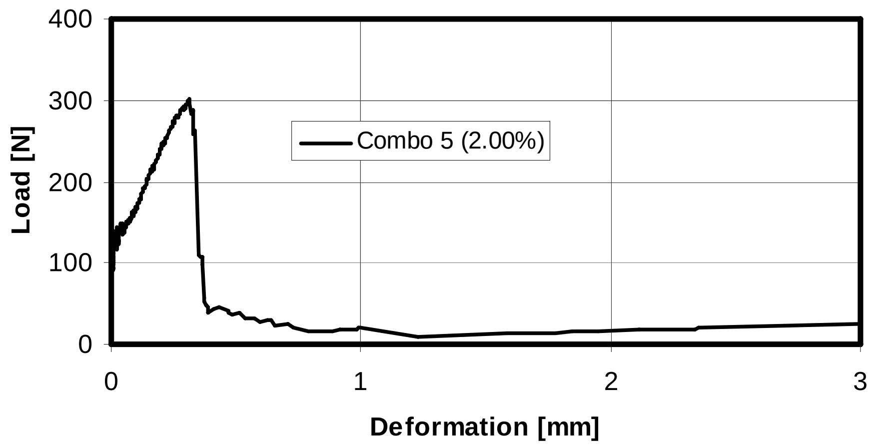


**Figure 4.8 Load displacement curve**

## Combo 5 (1% Fibers)

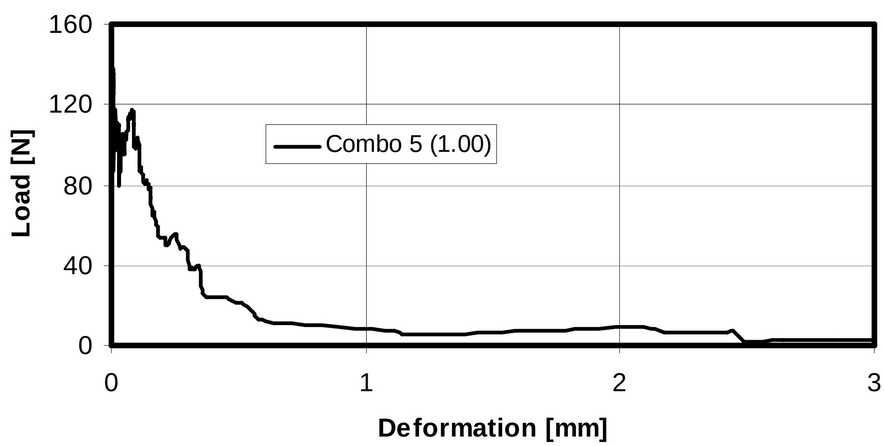


**Figure 4.9 Load displacement curve**

## Combo 6 (2% Fibers)

| | Radius (mm) | E (GPa) | ν, Poisson's ratio | G (MPa) | ft (MPa) | fc (MPa) |
|---|---|---|---|---|---|---|
| Matrix | 0.5 | 30 | 0.2 | 12500 | 5 | - |
| Interface | 0.1 | 50 | 0.333 | 18750 | 100 | -300 |
| Fiber | 0.022 | 41.1 | 0.35 | 15222 | 1640 | - |

**Table 4.9 Matrix-Fiber System Properties**

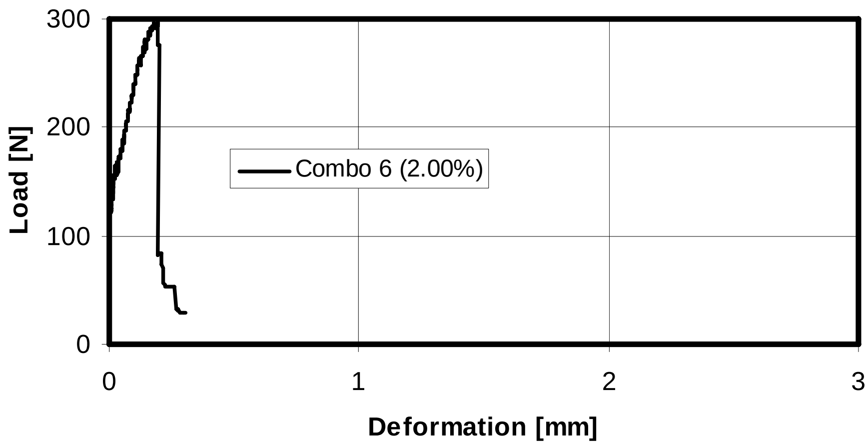


**Figure 4.10 Load displacement curve**

**Combo 6 (1% Fibers)**

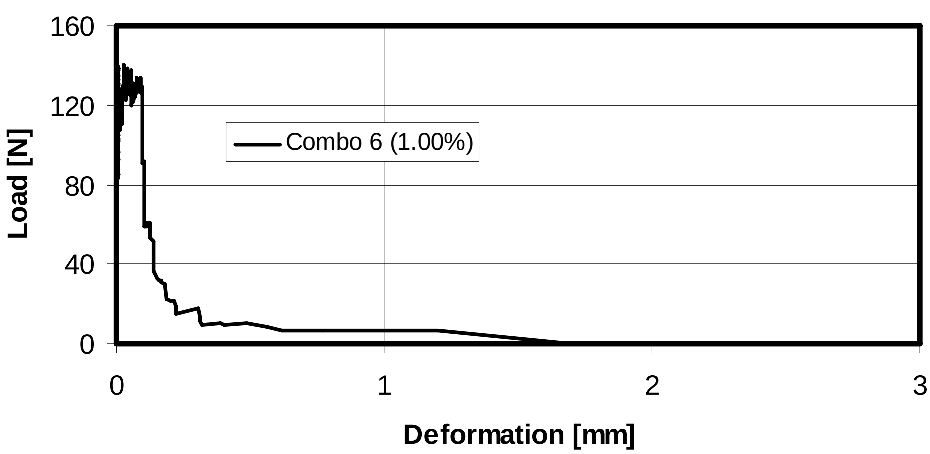


**Figure 4.11 Load displacement curve**

## 4.4.2 Second simulation

From the first simulation, it can be seen that the promising strain hardening behavior can be obtain from combination 2. In order to spread the crack to the other undamaged element, the softening behavior is introduced in the interface elements. In order to simulate softening behavior, the Interface Elastic modulus are made in 3 (three) steps decreasing value namely $E_1$ = 5000 MPa, $E_2$ = 3000 MPa, and $E_3$ = 1000 MPa. It is hoped that the deformation can be increased and larger load carrying capacity as well. The results can be shown as following.

**Combo 2 (2% Fibers)**

| | Radius (mm) | E (GPa) | ν, Poisson's ratio | G (MPa) | ft (MPa) | fc (MPa) |
|---|---|---|---|---|---|---|
| Matrix | 0.5 | 30 | 0.2 | 12500 | 5 | - |
| Interface | 0.1 | 5 | 0.333 | 1875 | 100 | -300 |
| Fiber | 0.022 | 41.1 | 0.35 | 15222 | 1640 | - |

**Table 4.10 Matrix-Fiber System Properties**

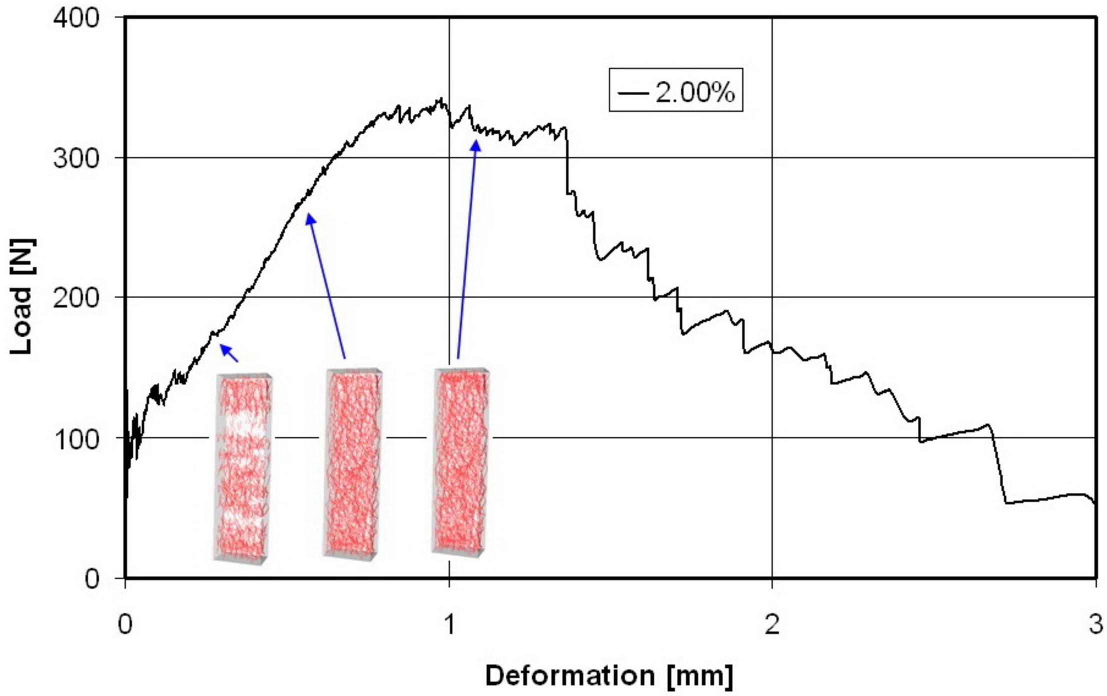


**Figure 4.12 Load displacement curve**

**Combo 2 (1% Fibers)**

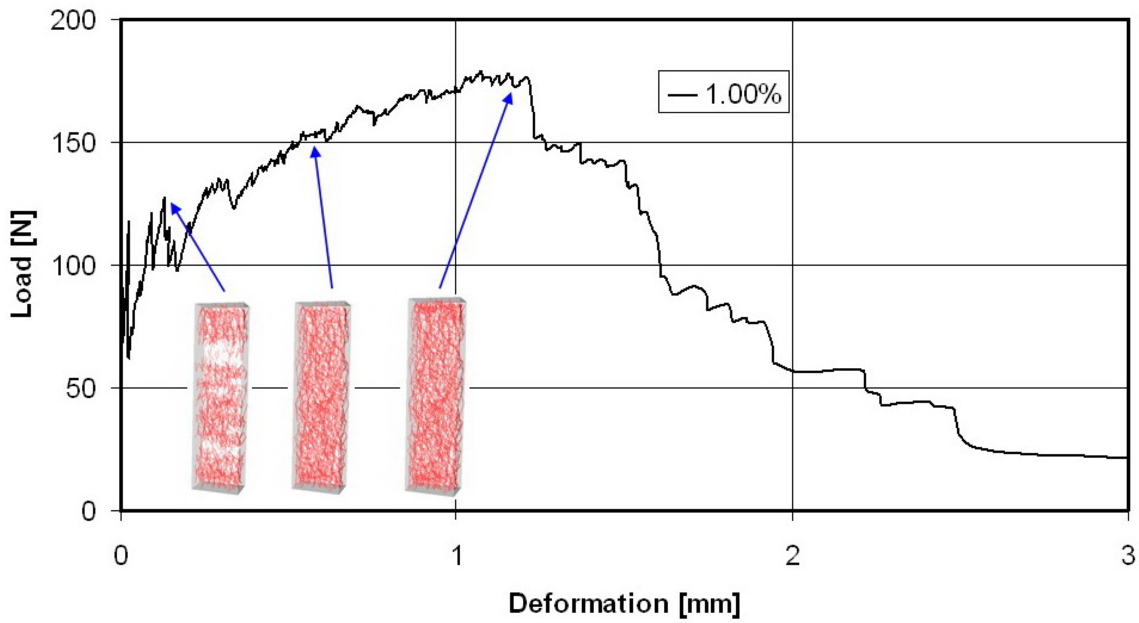


**Figure 4.13 Load displacement curve**

## 4.4.3 Third simulation

From the second simulation, it can be found that for 2%vol fiber fraction the load carrying capacity increase from 260 N to 340 N and its deformation increase from 0.7 mm to 1.3 mm. For 1%vol fiber fraction the load increases from 140 N to 180 N meanwhile the deformation increase from 0.6 mm to 1.3 mm. To gain optimum results, the interface softening behavior is introduced again to the interface. The idea is to distribute the crack to the undamaged part of the specimen. The Interface Elastic modulus are also made in 3 (three) steps decreasing value namely $E_1$ = 5000 MPa, $E_2$ = 1000 MPa, and $E_3$ = 150 MPa.

**Combo 2 (2% Fibers)**

| | Radius (mm) | E (GPa) | ν, Poisson's ratio | G (MPa) | ft (MPa) | fc (MPa) |
|---|---|---|---|---|---|---|
| Matrix | 0.5 | 30 | 0.2 | 12500 | 5 | - |
| Interface | 0.1 | 5 | 0.333 | 1875 | 100 | -300 |
| Fiber | 0.022 | 41.1 | 0.35 | 15222 | 1640 | - |

**Table 4.11 Matrix-Fiber System Properties**

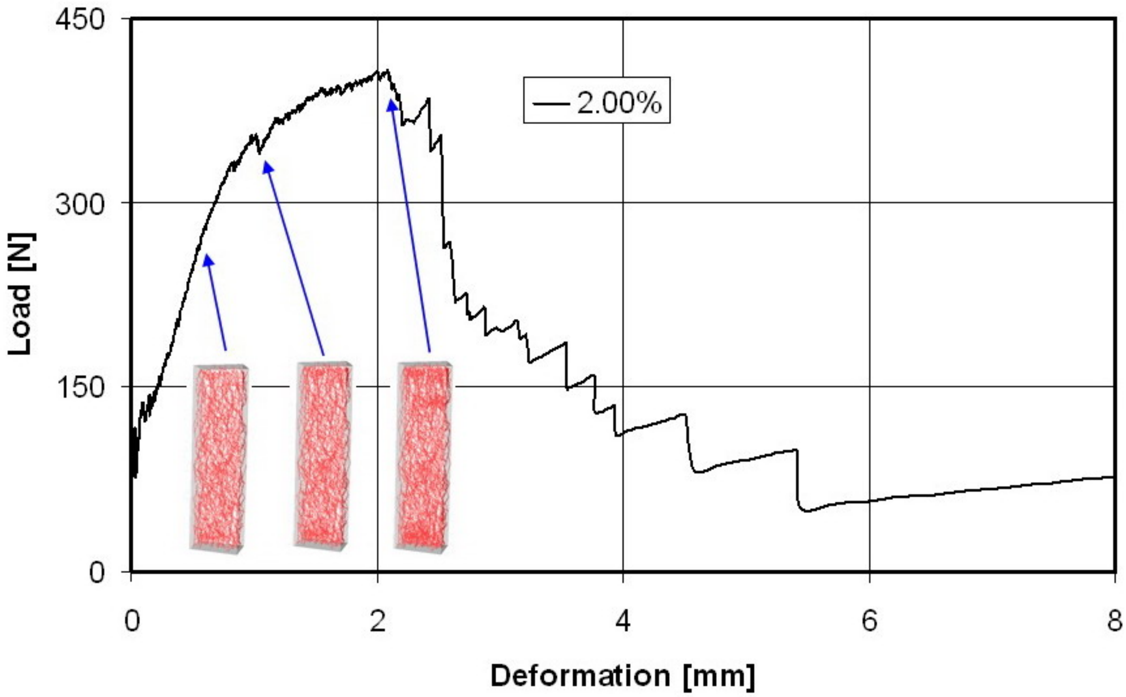


**Figure 4.14 Load displacement curve**

**Combo 2 (1% Fibers)**

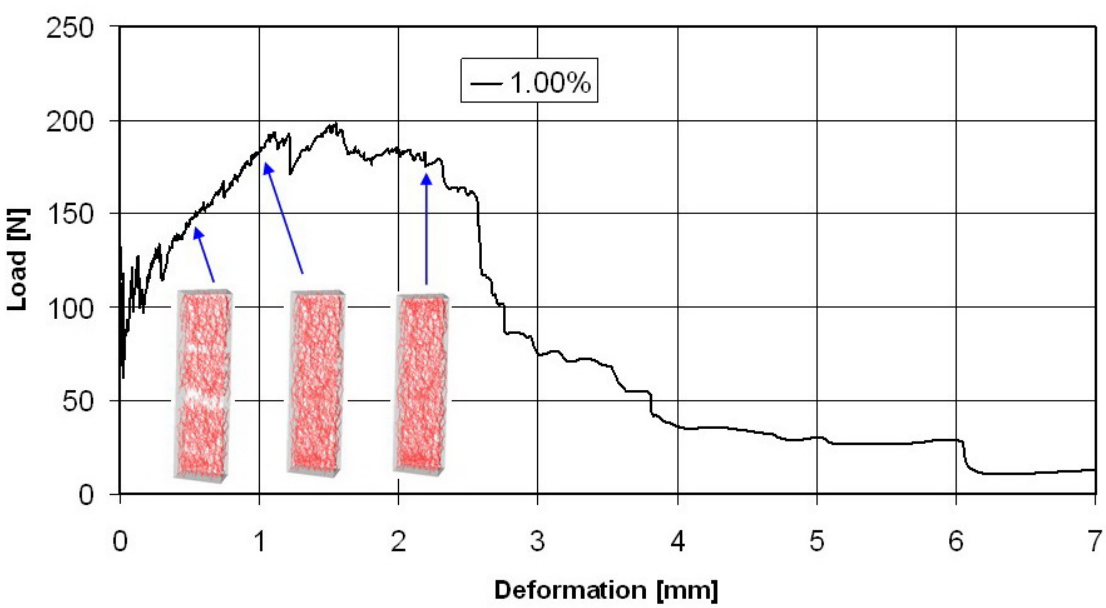


**Figure 4.15 Load displacement curve**

From the simulations above, it is found that for 2%vol fiber fraction the load carrying capacity increase significantly from 340 N to 410 N and the deformation increase from 1.3 mm to 3.0 mm. For 1%vol fiber fraction, the load increase from 180 N to 200 N and the deformation increase from 1.3 mm to 3.0 mm. It is quiet good result considering that the strain capacity is quiet high at around 10%.

## 4.5 Four point bending test

The simulation is carried out by using 8x5x30 specimen with fiber length 8 mm, and fiber volume fraction 1% and 2%. The matrix-fiber system properties from the uni-axial tensile test are used due to their good results.

| | Radius (mm) | E (GPa) | ν, Poisson's ratio | G (MPa) | ft (MPa) | fc (MPa) |
|---|---|---|---|---|---|---|
| Matrix | 0.5 | 30 | 0.2 | 12500 | 5 | - |
| Interface | 0.1 | 5 | 0.333 | 1875 | 100 | -300 |
| Fiber | 0.022 | 41.1 | 0.35 | 15222 | 1640 | - |

The general simulation procedure can be summarized as follow:

1. Generate 3D Random Lattice

In this step, the size of the tested specimen is defined. The lattice node and lattice beam for matrix element are generated.

2. Input the properties of the matrix element

The properties of matrix element are assigned in this stage.

3. Generate fiber element

Fiber elements are generated according to fiber volume fraction and fiber length.

4. Add fiber element to 3D Random Lattice

The fibers are introduced to 3D Random lattice system. Extra nodes are generated at each location where the fiber crosses the square grid. Bond beam which represents the interface element are generated between fiber nodes and the lattice nodes in the neighboring cell. The properties for fiber and interface elements are defined.

5. Make four point bending support

The position of the support and the applied external load are assigned.

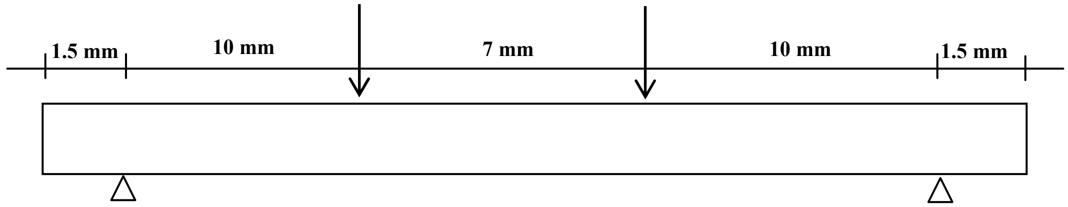


**Figure 4.17 Support and external load positions**

6. Make image for initial lattice element

The initial element images are made to check for the desired model.

7. GLAK Simulation

The lattice fracture simulations are done by using GLAK (Generalized Lattice Analysis Kernel). The procedure sequence in this step include performing a linear elastic analysis, calculating stresses in all the beams, removing one beam following strength criteria, and relaxing the displacements and removing next beam.

8. Make four point bending test graph from simulation results

The graph is plotted from the simulation result and determine the specimen behavior whether it is brittle, quasi-brittle or showing interesting strain-hardening failure.

9. Make image for damaged lattice element

This step is intended to investigate the crack patterns within the specimen which correspond to certain position in load deformation curve.

### 4.5.1 First simulation

The first simulation is done by using properties from the uni-axial tensile test, precisely from combination 2 which shows good strain capacity. The fiber volume fractions used are 1% and 2%. This first simulation is using linear interface properties. The simulation result can be seen as following

**Combo 2 (2% Fibers)**

| | Radius (mm) | E (GPa) | ν, Poisson's ratio | G (MPa) | ft (MPa) | fc (MPa) |
|---|---|---|---|---|---|---|
| Matrix | 0.5 | 30 | 0.2 | 12500 | 5 | - |
| Interface | 0.1 | 5 | 0.333 | 1875 | 100 | -300 |
| Fiber | 0.022 | 41.1 | 0.35 | 15222 | 1640 | - |

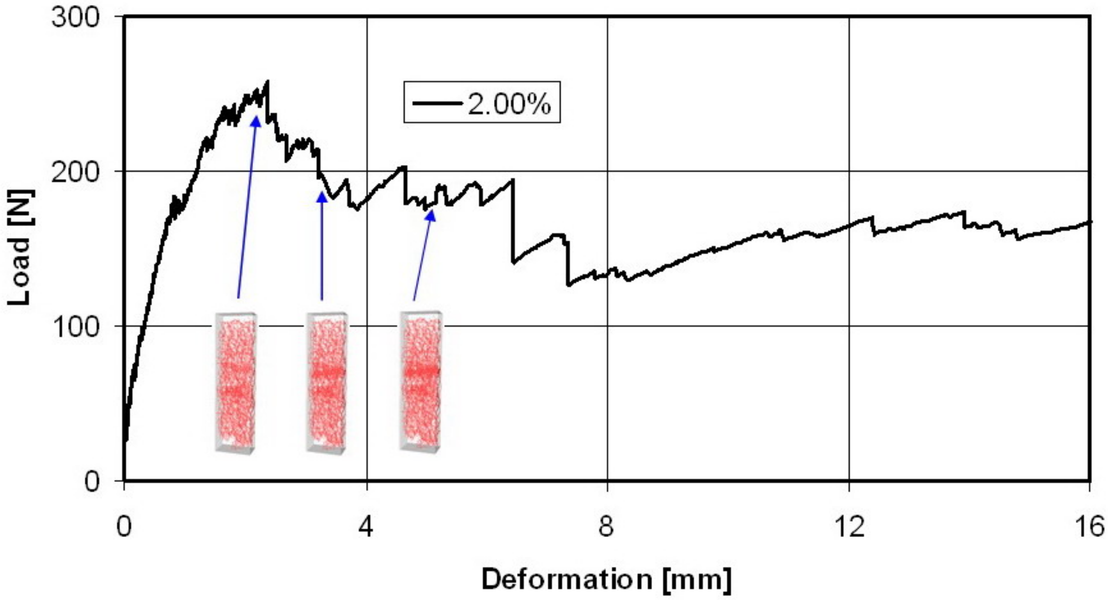


**Combo 2 (1% Fibers)**

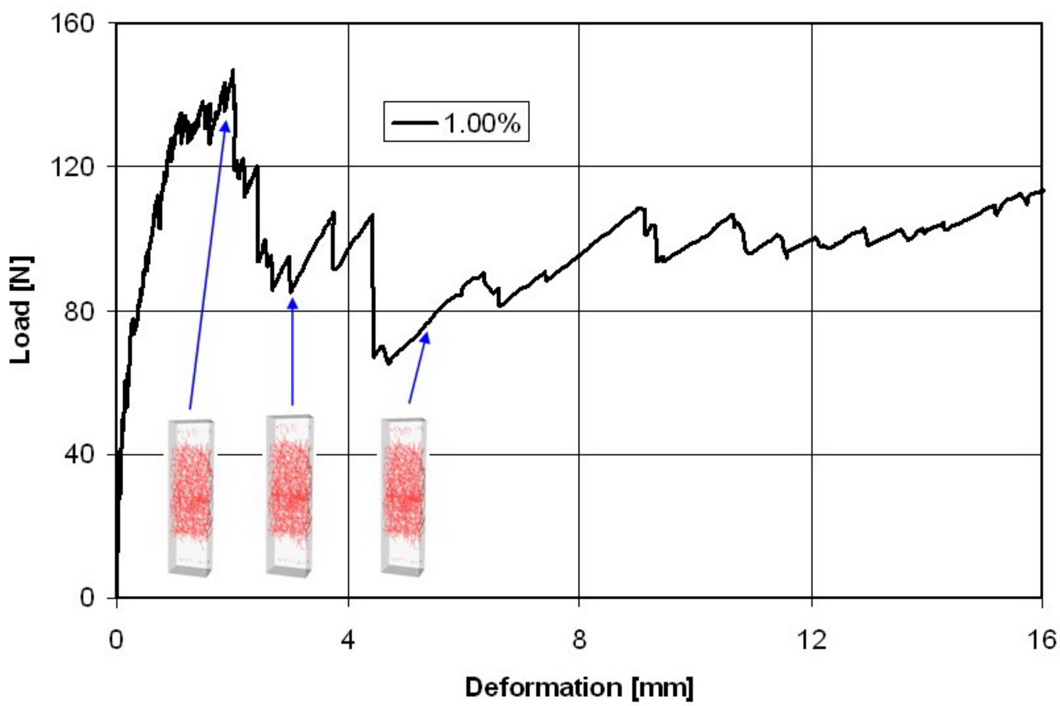


## 4.5.2 Second simulation

From the first simulation, it is obtained that there are still possibility to spread the crack to the other undamaged element. In order to do so, the softening behavior is introduced in the interface elements. This non-linear behavior is simulated by using 3 (three) steps decreasing value of the interface elastic modulus, namely E1 = 5000 MPa, E2 = 3000

MPa, and E3 = 1000 MPa. Hopefully, the deformation can be increased and larger load carrying capacity can be obtained. The results can be shown as following.

**Combo 2 (2% Fibers)**

| | Radius (mm) | E (GPa) | ν, Poisson's ratio | G (MPa) | ft (MPa) | fc (MPa) |
|---|---|---|---|---|---|---|
| Matrix | 0.5 | 30 | 0.2 | 12500 | 5 | - |
| Interface | 0.1 | 5 | 0.333 | 1875 | 100 | -300 |
| Fiber | 0.022 | 41.1 | 0.35 | 15222 | 1640 | - |

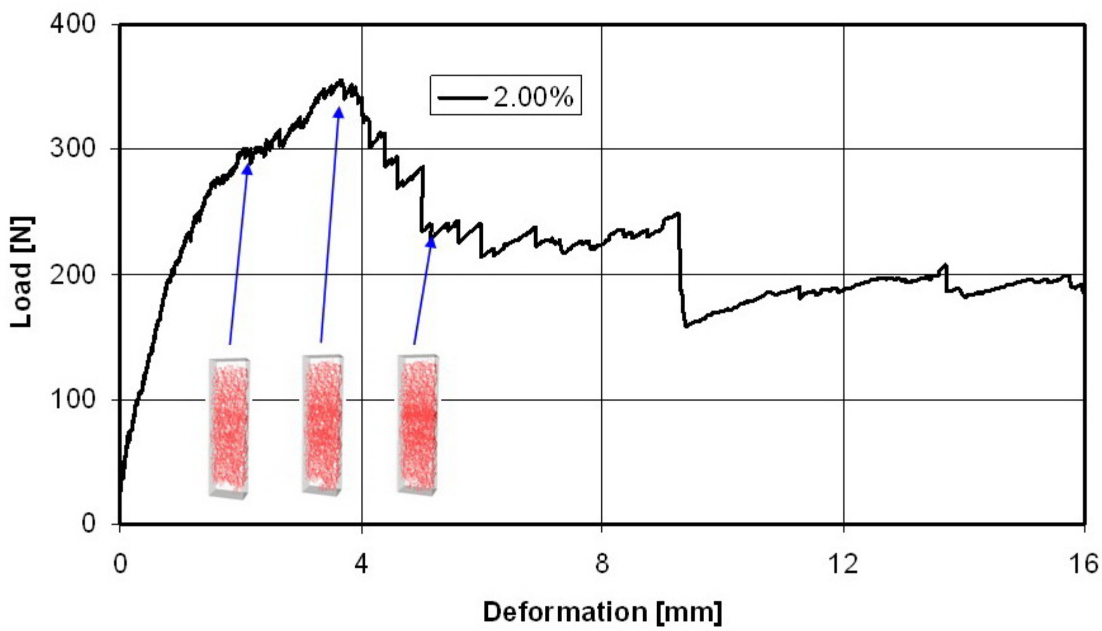

**Combo 2 (1% Fibers)**

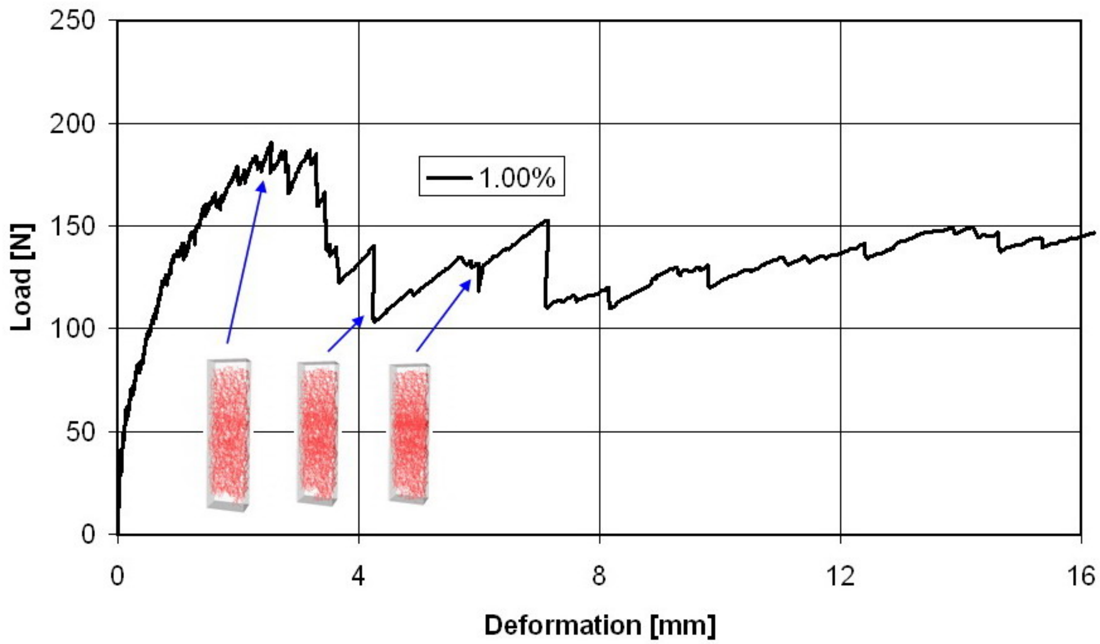


### 4.5.3 Third simulation

From the second simulation, it can be found that for 2%vol fiber fraction the load carrying capacity increase from 250 N to 340 N and its deformation increase from 2 mm to 4 mm. For 1%vol fiber fraction the load increases from 140 N to 180 N meanwhile the deformation increase from 2 mm to 3 mm. To gain optimum results, the interface softening behavior is introduced again to the interface. The idea is to distribute the crack to the undamaged part of the specimen. The Interface Elastic modulus are also made in 3 (three) steps decreasing value namely $E_1$ = 5000 MPa, $E_2$ = 1000 MPa, and $E_3$ = 150 MPa.

**Combo 2 (2% Fibers)**

| | Radius (mm) | E (GPa) | ν, Poisson's ratio | G (MPa) | ft (MPa) | fc (MPa) |
|---|---|---|---|---|---|---|
| Matrix | 0.5 | 30 | 0.2 | 12500 | 5 | - |
| Interface | 0.1 | 5 | 0.333 | 1875 | 100 | -300 |
| Fiber | 0.022 | 41.1 | 0.35 | 15222 | 1640 | - |

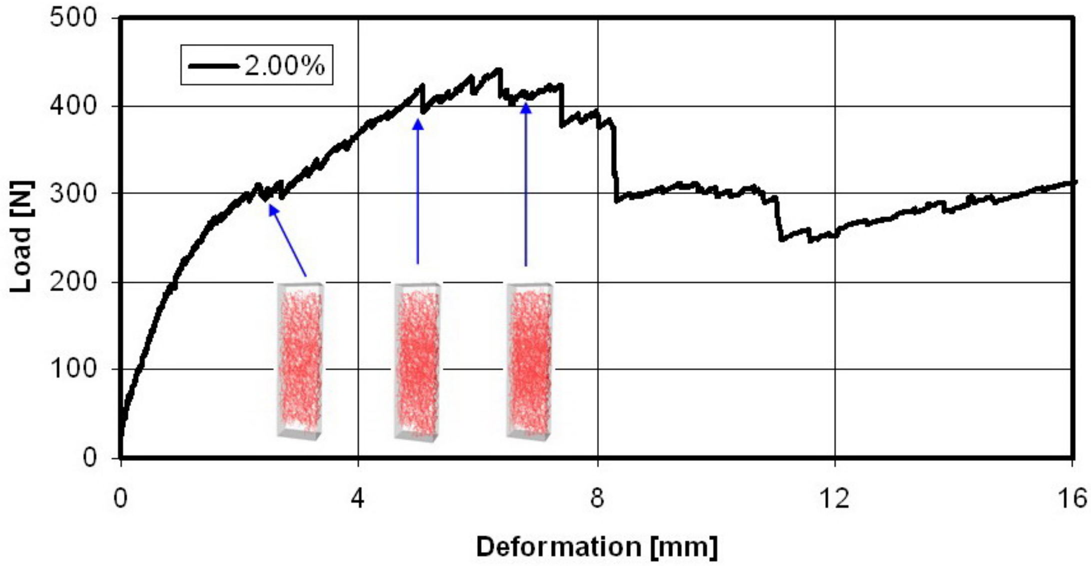


**Combo 2 (1% Fibers)**

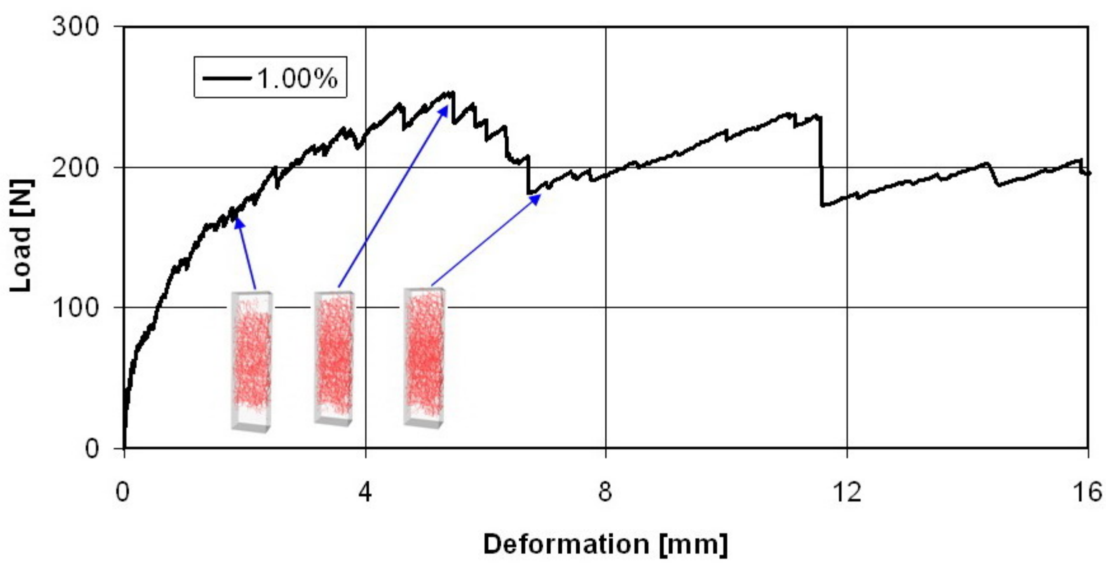


From the simulations above, it is found that for 2%vol fiber fraction the load carrying capacity increase significantly from 340 N to 410 N and the deformation increase from 4 mm to 8 mm. For 1%vol fiber fraction, the load increase from 180 N to 250 N and the deformation increase from 3 mm to 6 mm. It is quiet high result considering that the strain capacity is at around 26.7%.
In order to cross-check this high value it is necessary to simulate pull-out test using this specimen properties.

### 4.5.4 Pull-out test, cross-check simulation.

In this simulation, specimen 8x5x30 is used with 10 mm fiber embedment length. The element properties are as following.

| | Radius (mm) | E (GPa) | ν, Poisson's ratio | G (MPa) | ft (MPa) | fc (MPa) |
|---|---|---|---|---|---|---|
| Matrix | 0.5 | 30 | 0.2 | 12500 | 5 | - |
| Interface | 0.1 | 5 | 0.333 | 1875 | 100 | -300 |
| Fiber | 0.022 | 41.1 | 0.35 | 15222 | 1640 | - |

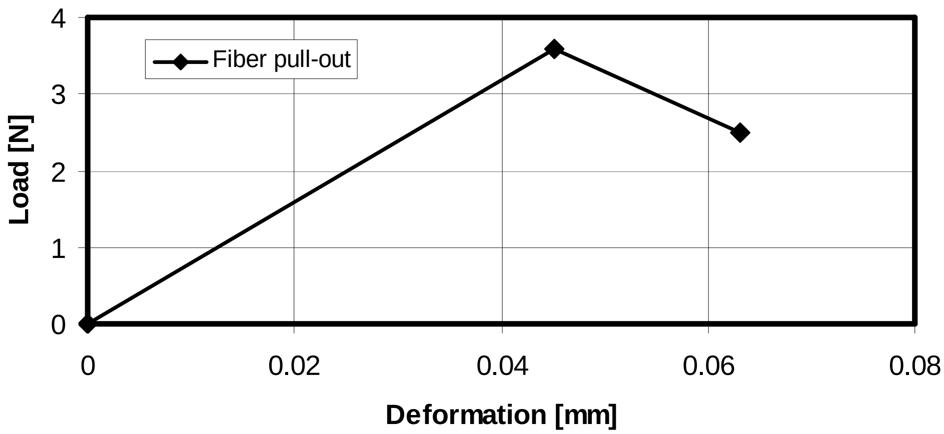


The simulation shows a brittle behavior. The fiber element breaks before it can bridge the load from the crack to the other undamaged element. It seems that the interface strength is quiet high. In order to spread crack to the other location, which resulting multiple cracking, the interface strength will be reduced systematically in which high strain capacity will be obtained.

After performing some simulation, the promising element properties are gained as following.

| | Radius (mm) | E (GPa) | ν, Poisson's ratio | G (MPa) | ft (MPa) | fc (MPa) |
|---|---|---|---|---|---|---|
| Matrix | 0.5 | 30 | 0.2 | 12500 | 5 | - |
| Interface | 0.1 | 5 | 0.333 | 1875 | 5 | -15 |
| Fiber | 0.022 | 41.1 | 0.35 | 15222 | 1640 | - |

The tensile strength ($f_t$) should be 5 MPa and the compression strength ($f_c$) at around -15 MPa.

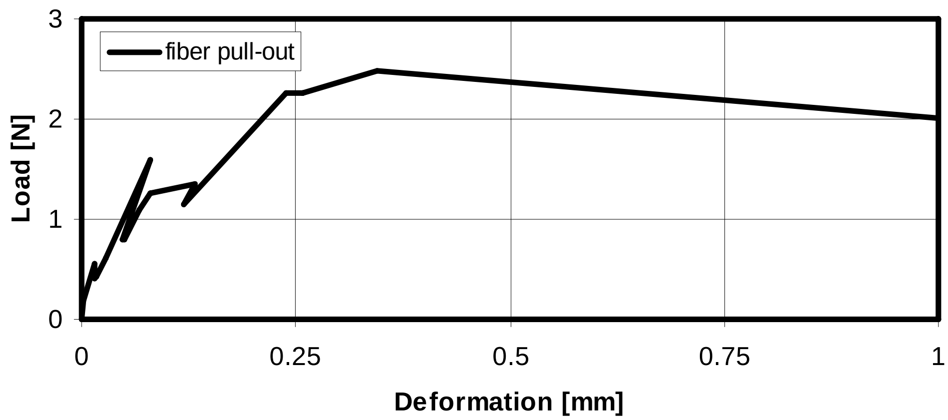


## 4.5.5 Four point bending test (input from fiber pull-out test), cross-checked simulations

The element properties from this fiber pull-out test are then used as an input for 4 (four point bending test.

### 4.5.5.1 First simulation

The first simulation is done by using properties from the fiber pull-out test, precisely from combination which shows good strain capacity. The fiber volume fractions used are 1% and 2%. This first simulation is using linear interface properties. The simulation result can be seen as following

**2% Fibers**

| | Radius (mm) | E (GPa) | ν, Poisson's ratio | G (MPa) | ft (MPa) | fc (MPa) |
|---|---|---|---|---|---|---|
| Matrix | 0.5 | 30 | 0.2 | 12500 | 5 | - |
| Interface | 0.1 | 5 | 0.333 | 1875 | 5 | -15 |
| Fiber | 0.022 | 41.1 | 0.35 | 15222 | 1640 | - |

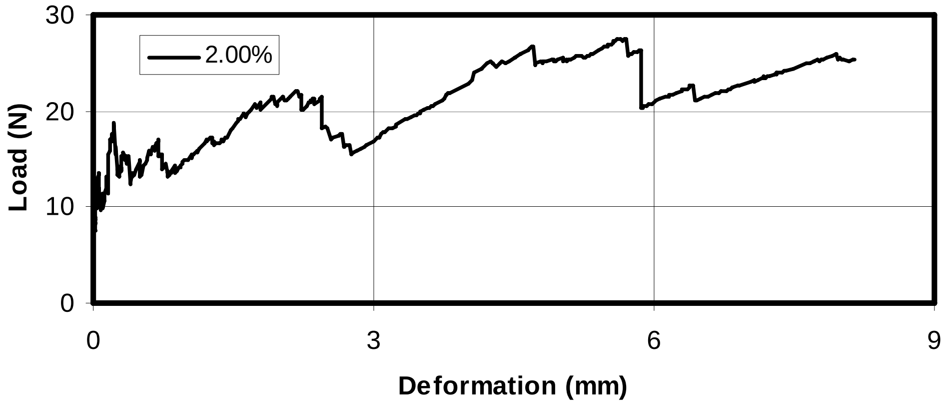


**1% Fibers**

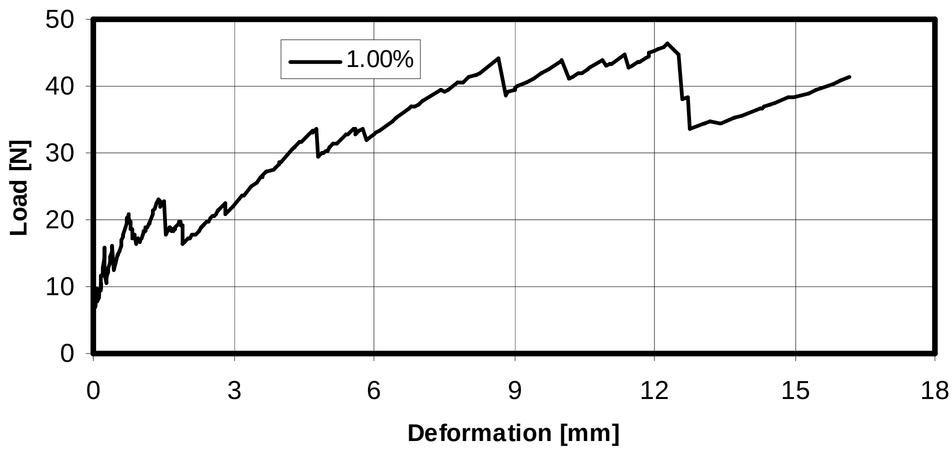


## 4.5.5.2 Second simulation

From the first simulation, it is obtained that there are still possibility to spread the crack to the other undamaged element. In order to do so, the softening behavior is introduced in the interface elements. This non-linear behavior is simulated by using 3 (three) steps decreasing value of the interface elastic modulus, namely E1 = 5000 MPa, E2 = 3000 MPa, and E3 = 1000 MPa. Hopefully, the deformation can be increased and larger load carrying capacity can be obtained. The results can be shown as following.

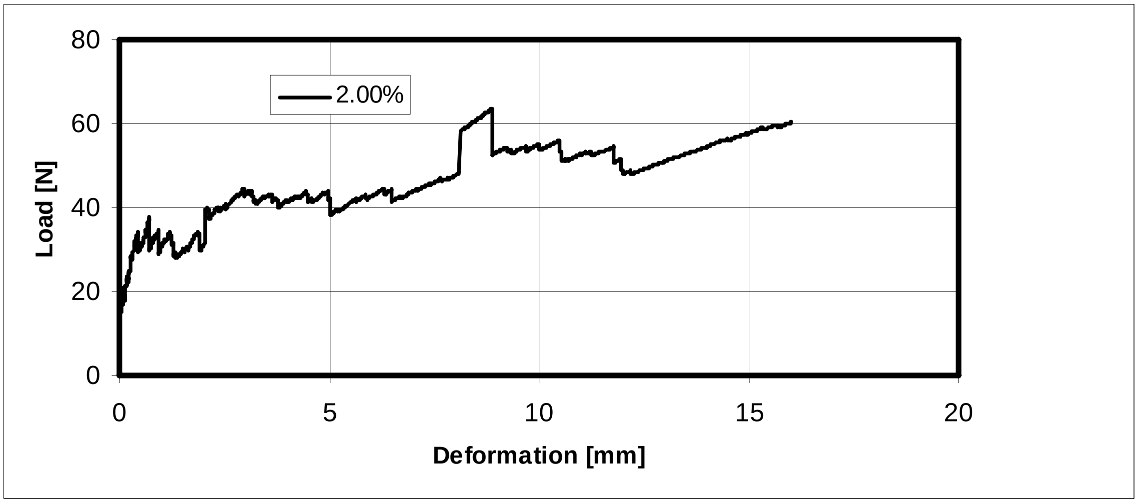


**2% Fibers**

| | Radius (mm) | E (GPa) | ν, Poisson's ratio | G (MPa) | ft (MPa) | fc (MPa) |
|---|---|---|---|---|---|---|
| Matrix | 0.5 | 30 | 0.2 | 12500 | 5 | - |
| Interface | 0.1 | 5 | 0.333 | 1875 | 5 | -15 |
| Fiber | 0.022 | 41.1 | 0.35 | 15222 | 1640 | - |

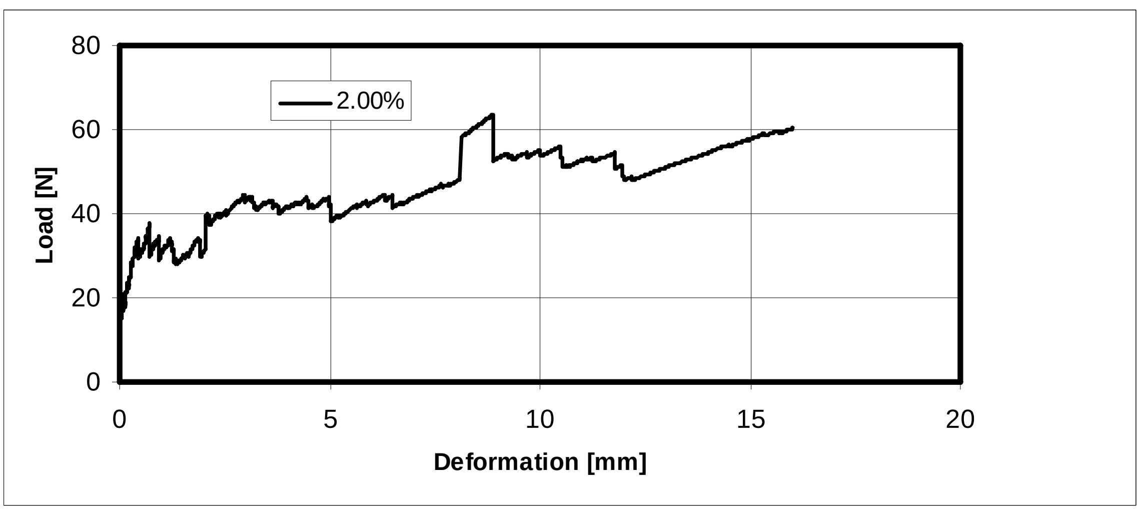

**1% Fibers**

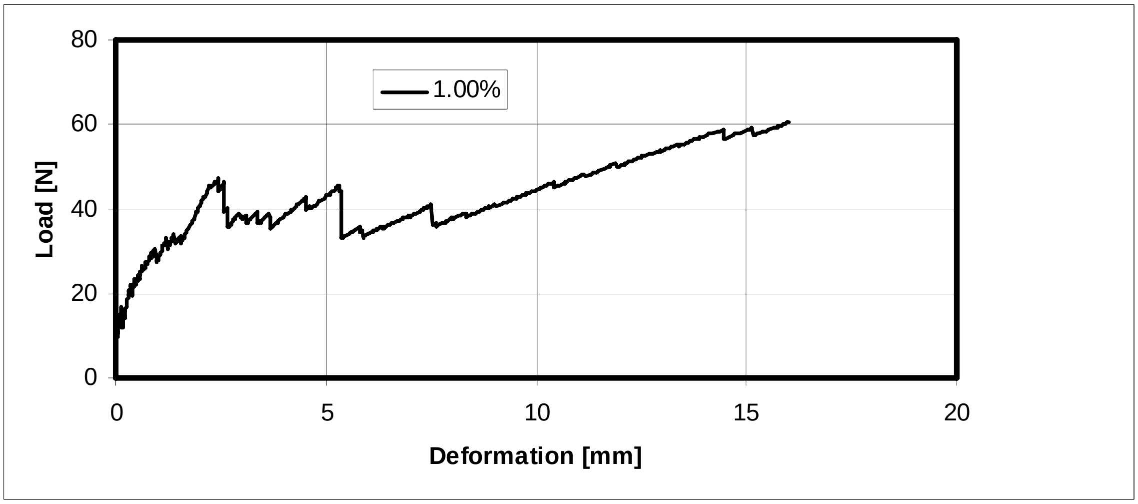


## 4.5.5.3 Third simulation

From the second simulation, it can be found that for 2%vol fiber fraction the load carrying capacity increase from 30 N to 60 N and its deformation increase from 2 mm to 4 mm. For 1%vol fiber fraction the load increases from 50 N to 60 N meanwhile the deformation increase from 2 mm to 3 mm. To gain optimum results, the interface softening behavior is introduced again to the interface. The idea is to distribute the crack to the undamaged part of the specimen. The Interface Elastic modulus are also made in 3 (three) steps decreasing value namely $E_1$ = 5000 MPa, $E_2$ = 1000 MPa, and $E_3$ = 150 MPa.

**2% Fibers**

| | Radius (mm) | E (GPa) | ν, Poisson's ratio | G (MPa) | ft (MPa) | fc (MPa) |
|---|---|---|---|---|---|---|
| Matrix | 0.5 | 30 | 0.2 | 12500 | 5 | - |
| Interface | 0.1 | 5 | 0.333 | 1875 | 5 | -15 |
| Fiber | 0.022 | 41.1 | 0.35 | 15222 | 1640 | - |

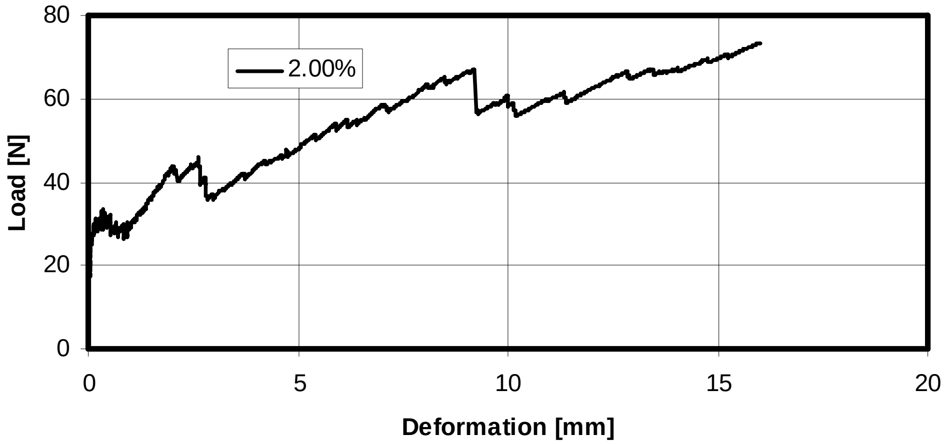


**1% Fibers**

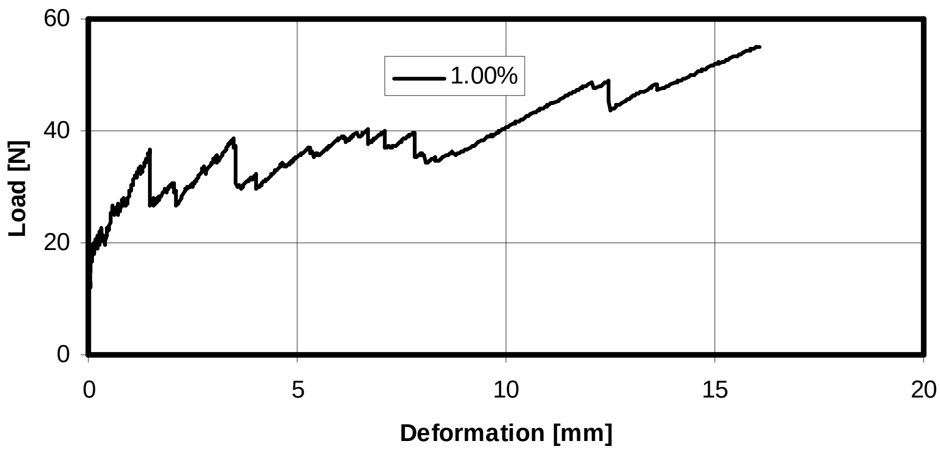


From the simulations above, it is found that for 2%vol fiber fraction the load carrying capacity increase significantly from 340 N to 410 N and the deformation increase from 4 mm to 8 mm. For 1%vol fiber fraction, the load increase from 180 N to 250 N and the deformation increase from 3 mm to 6 mm. It is quiet high result considering that the strain capacity is at around 26.7%.
In order to cross-check this high value it is necessary to simulate pull-out test using this specimen properties.

# Chapter 5 3D Lattice Analysis and Experimental Result Comparisons

This chapter compares the results from 3D lattice simulation with the experimental test qualitatively. The comparisons consist of single fiber test, uni-axial tensile test, and four point bending test.

## 5.1 Single fiber tensile test

As can be seen from Figure 5.1, there are three branches related with the load deformation curve. First branch shows initial elastic stretching of the fiber free length (the portion not embedded). The second branch is debonding stage. The third branch, a concave upward portion of the curve, indicates the slip hardening behavior.

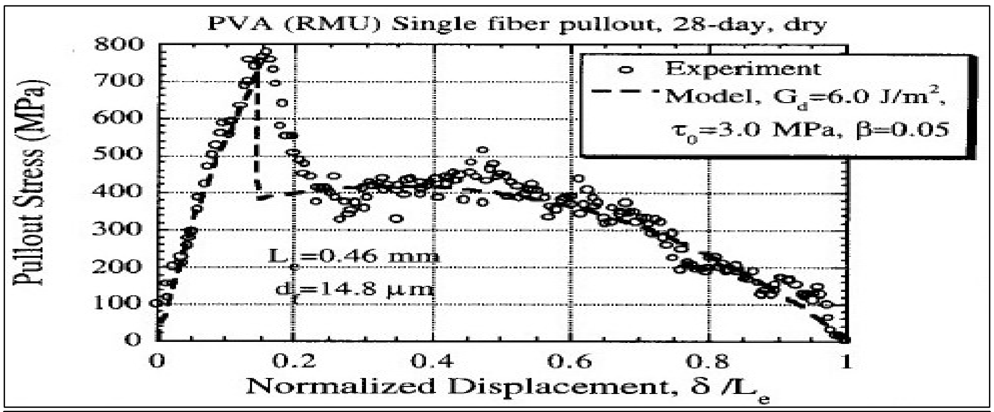


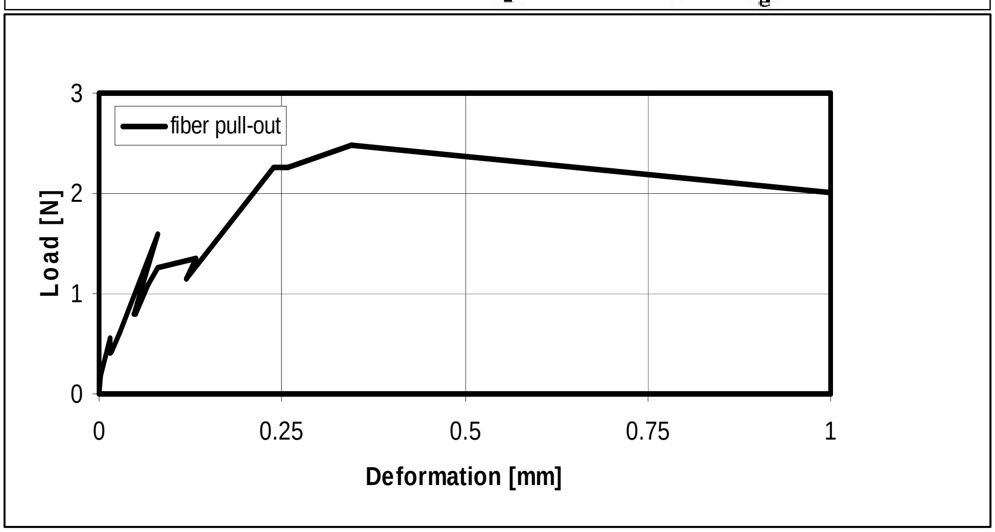


**Figure 5.1 Single fiber pull-out test: Test result (left) vs simulation result (right)**

Qualitatively, the simulation result show quiet similar behavior with the test results.

## 5.2 Uni-axial tensile test

Compared to experimental test results, the simulation tests show quiet promising higher value of strain capacity. It is also quiet interesting to be noticed that the fiber volume fraction gained from the simulations still applicable and economical.

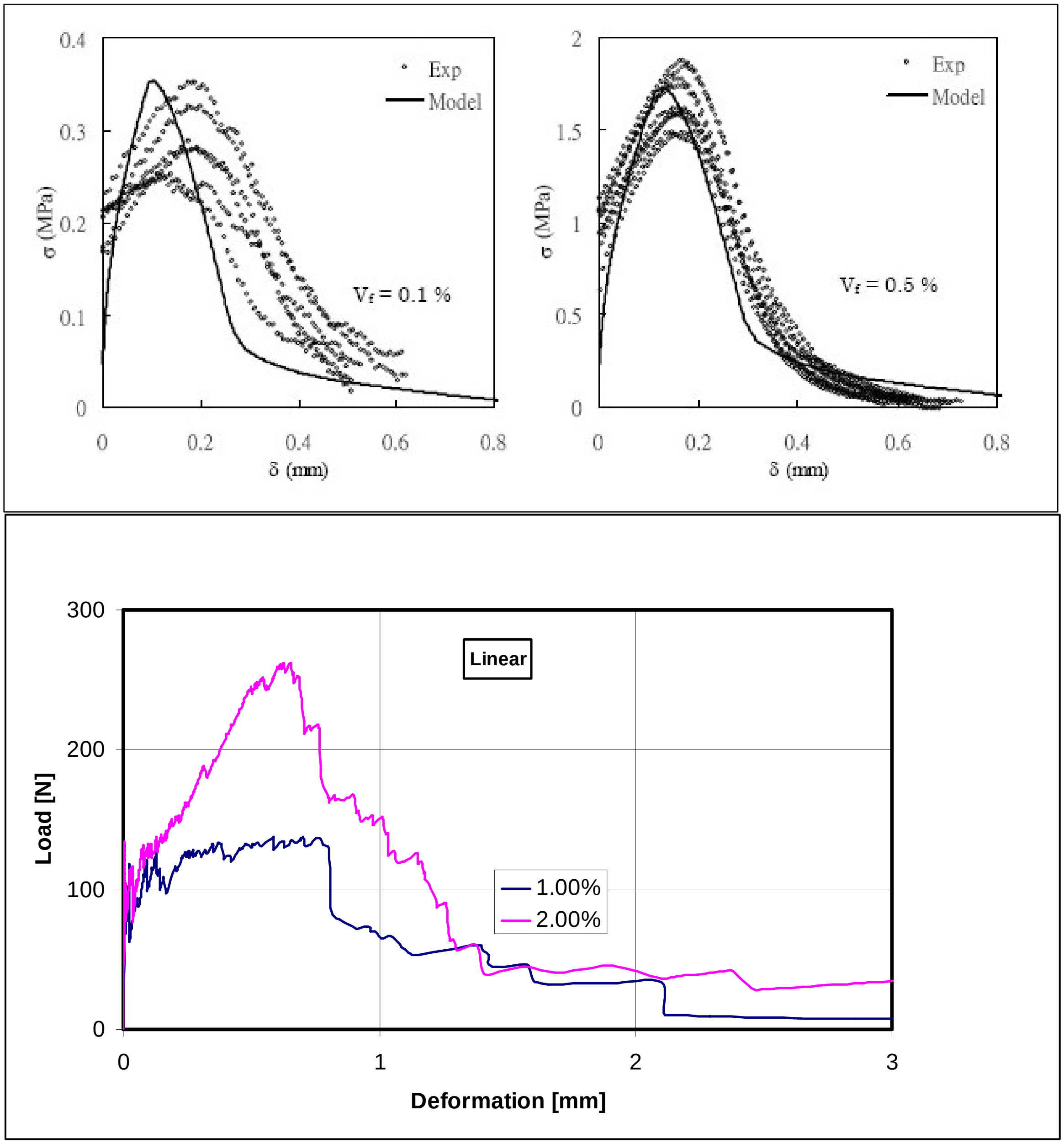


**Figure 5.2 Uni-axial tensile test: Test results (upper) vs simulation results (lower)**

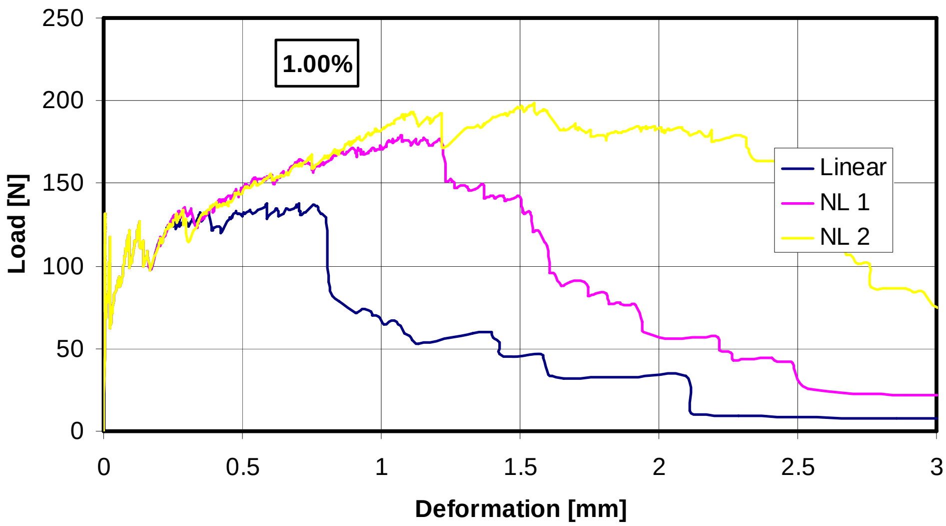


**Figure 5.3 Uni-axial tensile test – Non Linear Interface properties (1% fiber by volume)**

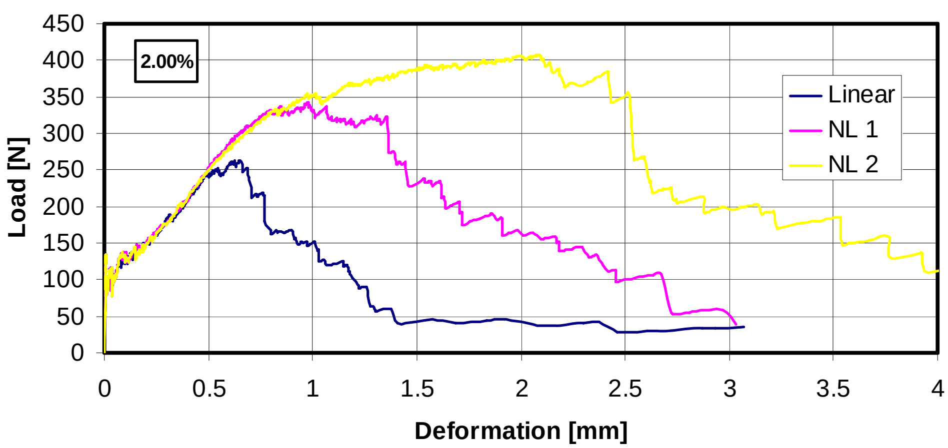


**Figure 5.4 Uni-axial tensile test – Non Linear Interface properties (2% fiber by volume)**

The use of interface softening (non-linear) properties is proved to be effective to increase the strain capacity of the simulation results. As can be seen form figure 5.3 and figure 5.4, the specimen has the strain capacity at around 10%.

## 5.3 Four point bending test

The results form the simulation tests show quiet higher value of strain capacity compare to experimental results. However, the failure behavior is relatively similar. These results has been cross-checked with that from fiber pull-out tests.

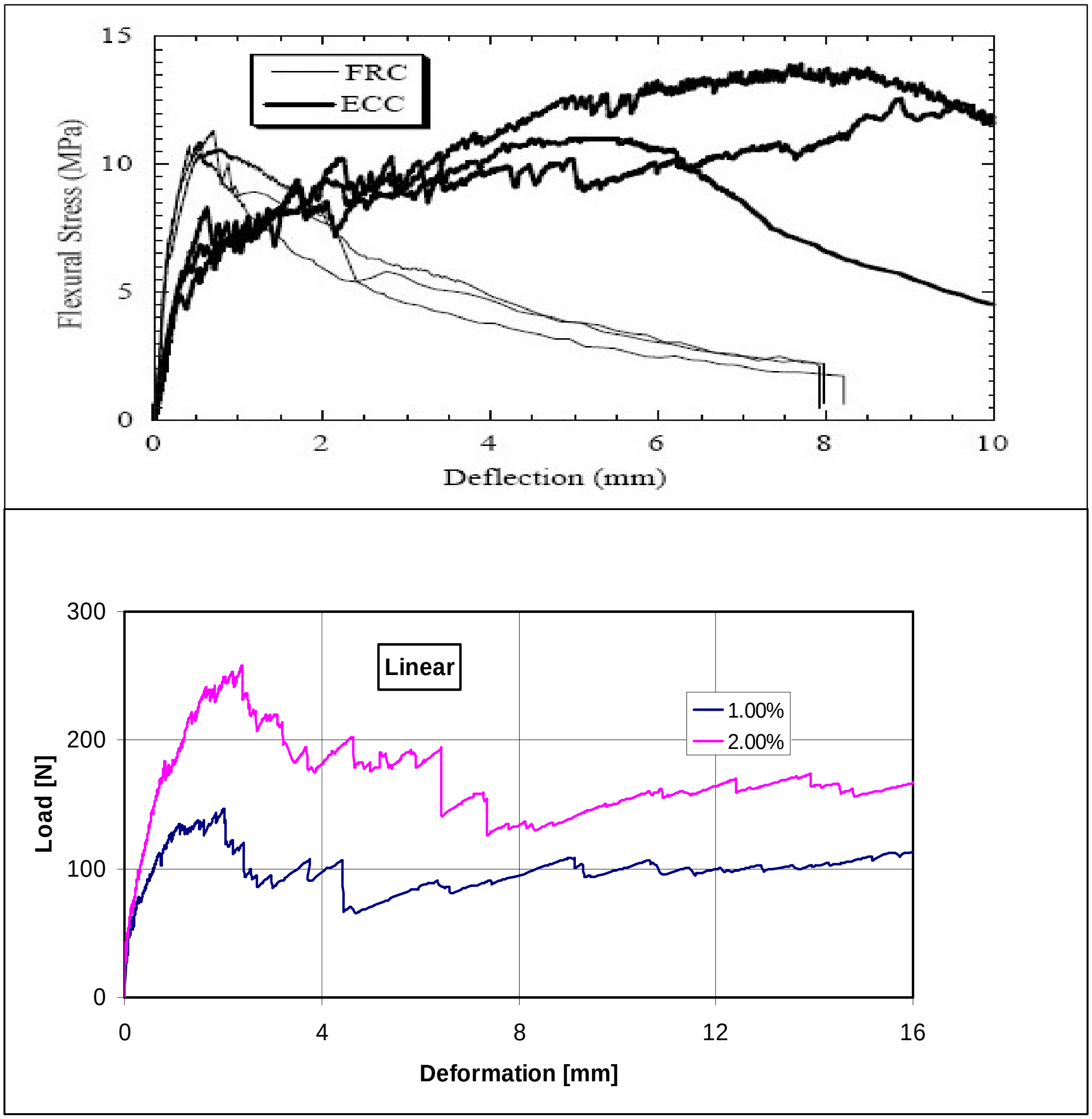


**Figure 5.5 Four Point Bending Test: Test results (upper) vs simulation results (lower)**

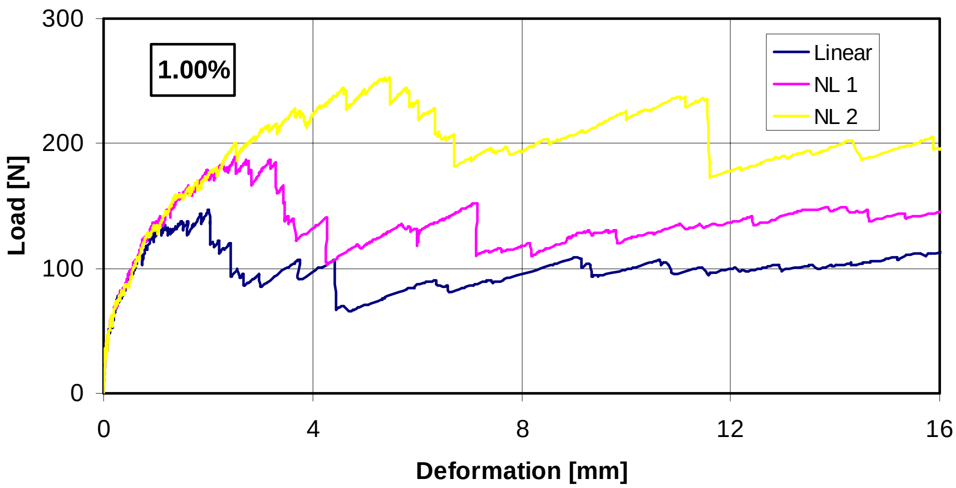


**Figure 5.6 Four Point Bending Test - Non Linear Interface properties (1% fiber by volume)**

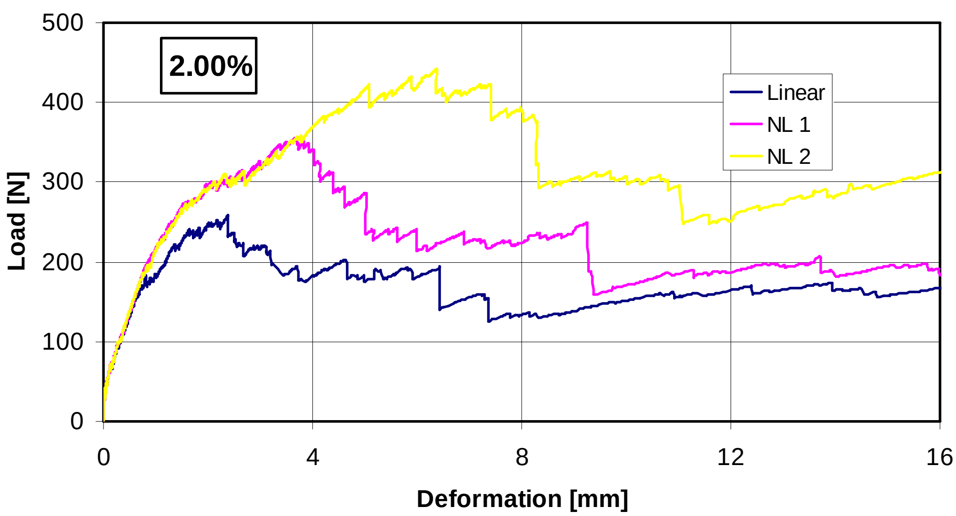


**Figure 5.7 Four Point Bending Test - Non Linear Interface properties (2% fiber by volume)**

The use of interface softening (non-linear) properties can increase the peak load carrying capacity. As can be seen form figure 5.6 and figure 5.7, the specimen peak load ranges from 100 N to 400 N.

# Chapter 6 Conclusions and Further Investigation

## 6.1 Summary of the MSc thesis project

In this MSc thesis project, an effort is made to simulate ductility aspect and fracture processes in fiber reinforced cementitious composites through 3D lattice fracture model at the meso-level.

This project consists of three main simulations, namely Single fiber pull-out test, uni-axial tensile test, and four point bending test, the role of each is to cross-check each other and to compare the curve behavior.

The simulation itself consists of three main steps. First step is pre-processing that generates 3D Random lattice and incorporates element properties in the model. Second step is kernel that simulates and analyzes the model. The last step is post-processing that have a role in interpretation of the simulation results. All these steps are carried out according to Finite Element Method.

During the simulation, the softening behaviors (non-linear properties) of interface elements are also studied, in order to increase strain capacity of the specimen.

Similar to the analytical micromechanical approach, fiber, matrix, and interface parameter are also important and influencing this meso-scale simulation results.

In general, the procedure carried out to simulate ductility behavior is as following.

1. Set the diameter of the matrix element such that the matrix elastic modulus is similar to lattice model elastic modulus
2. Use matrix properties corresponding to the chosen matrix elastic modulus [30].
3. Choose realistic fiber properties that are readily available in the market [32, 33].
4. The interface properties depend on its radius, elastic modulus, tensile strength, and compressive strength. These are varied and values that yield a large interface ductility are selected. From the simulation, it is found that the interface radius should have the same metric-prefix with the matrix radius. The interface elastic modulus should have one unit lower metric-prefix compare to that from matrix. The interface tensile and compressive strength should have two unit higher metric-prefix compare to that from matrix. Their value should also be set to 1:3 ratio.
5. The resulting simulation is plotted in load-deformation graph. The ductile behavior can be found from the graph that shows large strain capacity.
6. Introduce softening (non-linear) behavior to interface elastic modulus and run the analysis again. This step is taken in order to optimize composite ductility behavior.

During the current simulation, brittle behavior is obtained from earlier fiber breaking before the composite is able to show large strain capacity. The fibers are quiet important to bridge the load from the damaged part to the undamaged part. Most of the time early fiber breaking is due to stronger interface elements compared to that of fiber elements.

## 6.2 Known limitations and possible solutions

The proposed procedure to design ductile fiber reinforced materials can be improved further in several aspects.

First of all, it is found that the simulation results for bending test are not in accordance with the experimental results. It is suggested to use the similar specimen size and properties with the experimental tests.

For this time being, the interface properties can only be predicted. In order to control them, one will need better understanding of the relation between matrix and interface properties. This can be obtained through simulation within the other scale (nano-, micro-, and macro-scale) and also check them with several laboratory tests.
Another drawback of the current simulation is that the demand for computational time is so huge that make it impossible to get sufficient comparative results within a reasonable period. A newly developed parallel computing based on GPU (Graphics Processing Units) Cluster Computing recently proved to be efficient and effective for large simulations and computing for finite element applications. It appears that for relatively low costs one can obtain supercomputer performance [34].

## 6.3 Further investigation

In this research project, only meso-scale is taken into account during the simulations. In order to realize the Integrated Structures and Materials Design (ISMD) concept into practice, therefore bridge the gap between structural engineers and material engineers, it is quite important to carry out the simulation also in multi (nano-, micro-, and macro-) scale. The experimental research in that respective level is also necessary to guarantee that the behavior of structural element (macro-level) is acting similarly to specimen behavior from the tailoring processes in multi-scale.

## References


[1] Lomborg, B., "The Skeptical Environmentalist: Measuring the Real State of the World", 17th printing, Cambridge University Press, 2006.

[2] U.S Geological Survey, "Minerals commodity summary - cement - 2008", USGS 2009, http://minerals.usgs.gov/minerals/pubs/commodity/cement/mcs-2008-cemen.pdf. (March 2009).

[3] Mehta, P.K. and Monteiro, P., "Concrete: Structure, Properties, and Materials", 2nd edition, Prentice-Hall, Inc., 1993

[4] Mehta, P.K., Monteiro, P., "Concrete: Microstructure, Properties, and Materials", The McGraw-Hill Companies, Inc., 2006.

[5] Leung, C.K.Y. and Li, V.C., "Application of a two-way debonding theory to short fiber composites", Composites, July 1990.

[6] Li, V.C., C. Wu, S. Wang, A. Ogawa, and T. Saito, Interface Tailoring for Strain-Hardening Polyvinyl Alcohol-Engineered Cementitious Composite (PVA-ECC), ACI Material Journal, V. 99, No. 5, September-October 2002.

[7] Li, V.C., On Engineered Cementitious Composites (ECC) – A review of the Material and Its Applications, Journal of Advanced Concrete Technology Vol. 1, No. 3, 215-230, 2003.

[8] Matsumoto, T. and Mihashi, H., JCI-DFRCC Committee "DFRCC Terminology and Application Concepts" *Journal of Advanced Concrete Technology*, Vol. 1 No. 3, 335-340. (2003).

[9] Naaman, A.E., and Reinhardt, H.W., "Characterization of High Performance Fiber Reinforced Cement Composites - HPFRCC", High Performance Fiber Reinforced Cement Composites (HPFRCC 2), pp. 1-23, 1996.

[10] Li, V.C., and Fischer, G. "Reinforced ECC – An evolution from Materials to Structures.", in Proceedings on CD, session 5, Paper K-13, Osaka, Japan, Fib 2002.

[11] Li, V.C, "Integrated Structures and Materials Design", Materials and Structures, RILEM, pp1 – 10, Jan 2006.

[12] Li, V.C., "Performance driven design of fiber reinforced cementitious composites", in Proceedings of 4th RILEM International Symposium on Fiber Reinforced Concrete, Ed. R.N. Swamy, Chapman and Hall, 12-30, 1992

[13] Shah, S.P. and Ouyang, C., "Toughening Mechanisms in Quasi-Brittle Materials", J. Eng. Mater. Technol. July 1993 Volume 115, Issue 3, 300 (8 pages)

[14] Lin, Z., Kanda, T., and Li, V.C., "On interface property characterization and performance of fiber-reinforced cementitious composites", Concrete Science and Engineering, Vol.1, pp.173-174, 1999.

[15] Li, V.C. and Leung, C.K.Y., "Steady state and multiple cracking of short random fiber composites", ASCE Journal of Engineering Mechanics, 118 (1992) 2246-2264

[16] Li, V.C. and Wu, H.C., "Conditions for pseudo strain-hardening" in "Fiber Reinforced Brittle Matrix Composites", Journal of Applied Mechanics Rev.45 (8) (1992) 390-398.

[17] Lin, Z. and Li, V.C., "Crack bridging in fiber reinforced cementitious composites with slip-hardening interfaces", Journal of the Mechanics and Physics of Solids 45 (5) (1997) 763-787

[18] Li, V.C., Engineered Cementitious Composites (ECC) – Tailored Composites through micromechanical modeling, in Fiber Reinforced Concrete: Present and the

Future edited by N. Banthia, A. Bentur, A. and A. Mufti, Canadian Society for Civil Engineering, Montreal, 1998, pp. 64-97.
[19] Beltran, M.G.S. and Schlangen, E., "Wood fiber reinforced cement matrix: a micromechanical based approach", Key Engineering Materials Vol. 385-387 (2008) pp 445-448.
[20] Li, V.C., "Post-crack scaling relations for fiber reinforced cementitious composites", ASCE Journal of Materials in Civil Engineering, 4 (1), 41-57 (1992)
[21] Li, V.C., Stang, H. and Krenchel, H., "Micromechanics of crack bridging in fiber reinforced concrete", Journal of Materials and Structures, 26, 486-494 (1993)
[22] Yang, E. Wang S., Yang, Y., and Li, V.C., "Fiber-Bridging Constitutive Law of Engineered Cementitious Composites", Journal of Advanced Concrete Technology, Vol. 6, No. 1, 181-193, February, 2008
[23] Wu, C., "Micromechanical Tailoring of PVA-ECC for Structural Applications", PhD thesis, Department of Civil and Environmental Engineering, University of Michigan, Ann Arbor, Mich., Jan., 2001.
[24] Li, V.C., Wang, S., and Wu, C., "Tensile Strain Hardening Behavior of PVA-ECC", ACI Material Journals, V.98, No. 6 , Nov.-Dec. 2001, pp. 483-492.
[25] Lin, Z. and Li, V.C., "Crack bridging in fiber reinforced cementitious composites with slip-hardening interface", J. Mech. Solids 45 (5) 763-787, 1997
[26] Wang, Y., Li, V.C., and Backer, S., "Modeling of fiber pull-out from a cement matrix", Int'l. J. Cement Comp. Lightweight Concrete 10 (3) 143-149, 1988
[27] Yang, E., Wang, S., Yang, Y., and Li, V.C., "Fiber-bridging constitutive law of engineered cementitious composites", Journal of advanced concrete technology, vol. 6, No.1, 181-193, February 2008.
[28] H. Stang, V.C. Li, Classification of Fiber Reinforced Cementitious Materials for Structural Applications, in 6th RILEM Symposium on Fiber-Reinforced Concrete (FRC) – BEFIB 2004, 20 – 22 September 2004, Varenna, Italy, pp 197-218.
[29] E. Schlangen, Z. Qian, M.G. Sierra Beltran, and J. Zhou, Simulation of Fracture in Fiber Cement-based Materials with a Micromechanical Lattice Model, in 12th International Conference on Fracture, July 12-17, 2009, Ottawa, Canada.
[30] H. Prabowo, 3D Lattice Fracture Simulation of Single Fiber Cement based Composites Pull-out Test, Additional MSc Thesis, TU Delft, 2009
[31] Z. Qian, 3D Lattice Analysis of Cement Paste, MSc-Thesis, Delft University of Technology, The Netherlands, 2008.
[32] C. Redon, V.C. Li, C. Wu, H. Hoshiro, T. Saito, A. Ogawa, Measuring and Modifying Interface Properties of PVA Fibers in ECC Matrix, Journal of Materials in Civil Engineering, Nov/Dec 2001
[33] L.D. Nielsen, H. Stang, P.N. Poulsen, Micromechanical Analysis of Fiber Reinforced Cementitious Composites, Journal of Advanced Concrete Technology, Vol. 5, No.3, 373-382, October, 2007
[34] Stefan Turek, Dominik Göddeke, Christian Becker, Sven Buijssen and Hilmar Wobker, UCHPC - UnConventional High Performance Computing for Finite Element Simulations, International Supercomputing Conference, Dresden, June 2008

## About the Project

The MSc thesis project was started in January 2009 and completed in July 2009, which lasted for seven months.

This project was carried out at the Microlab, Faculty of Civil Engineering and Geosciences, Delft University of Technology, the Netherlands.

The committee members of this project are Prof. dr. ir. Klaas van Breugel, Dr. ir. H.E.J.G. Schlangen, Dr. ir. P.C.J. Hoogenboom, ir. Z. Qian, and Ir. Lambert Houben.

All 3D Lattice fracture simulations carried out in this thesis were based on GLAK (Generalized Lattice Analysis Kernel).